DEUTSCHES ELEKTRONEN-SYNCHROTRON DESY

DESY 81-070
October 1981

EVIDENCE ON THE GLUON

by

P. Söding

NOTKESTRASSE 85 · 2 HAMBURG 52

To be sure that your preprints are promptly included in the
HIGH ENERGY PHYSICS INDEX ,
send them to the following address (if possible by air mail) :

DESY
Bibliothek
Notkestrasse 85
2 Hamburg 52
Germany

DESY 81-070
October 1981

Evidence on the Gluon*

P. Söding
Deutsches Elektronen-Synchrotron DESY, Hamburg

Abstract

The production of hard noncollinear gluons in short distance processes is discussed, with emphasis on recent results from e^+e^- interactions. The jet phenomena observed in the e^+e^- continuum and in Υ decay are consistently described as due to the emission of QCD gluons while alternative explanations fail. The vector and color-nonsinglet nature of the radiated quanta is directly verified.

* Invited talk presented at the PARTICLES AND FIELDS 1981 Conference: Testing the Standard Model; held at the Santa Cruz Institute for Particle Physics, September 1981

1. Introduction

The first circumstantial experimental evidence for gluons came from deep-inelastic electron-nucleon scattering[1]. In the framework of the quark parton model, the smallness of the integral

$$\int_0^1 F_2(x)dx = \int_0^1 \sum_i e_i^2 x\,[q_i(x) + \bar{q}_i(x)]\,dx$$

of the structure function for protons and neutrons led to the conclusion that the total fraction

$$\int_0^1 \sum_i x\,[q_i(x) + \bar{q}_i(x)]\,dx$$

of the nucleon's momentum carried by quarks and antiquarks is only about one-half[2]. The missing momentum had to be carried by neutral partons. These were thought to be the gluons, the quanta of the field by which the quarks interact.

In field theories of the strong interaction the total amount of momentum carried by gluons in the nucleon is expected to depend on the four-momentum q of the probing current. As $|q^2|$ increases the quarks in the nucleon get increasingly resolved into systems composed of quarks accompanied by gluons; consequently the fractional momentum x found on quarks and antiquarks decreases[3]. When scaling violation, i.e. q^2 dependence of the structure functions, was observed it therefore was interpreted as evidence for the predominantly collinear emission of gluons by quarks in the nucleon[4] (Fig. 1a). This gluonic radiative correction causes however only a $\log q^2$ variation that has to be separated from other, stronger q^2 dependences. Only recently a consistent picture is emerging from the various deep-inelastic scattering experiments, further supported by mounting evidence for noncollinear gluon radiation reflected in a broadening of the final hadron jet[5].

The first rather direct evidence for gluons was found in the observation at PETRA that the reaction

$$e^+e^- \to \text{hadrons} \qquad (1)$$

produces, besides a dominant two-jet structure, a certain fraction of three-jet events[6]. This suggested that a hard noncollinear gluon radiated by one of the pair-produced quarks can manifest itself in a distinct jet of hadrons (Fig. 1b), as predicted on the basis of Quantum Chromodynamics (QCD) by Polyakov[7] and by J. Ellis et al.[8].

Independent evidence for gluon jets came from the observation at DORIS that the decay

$$\Upsilon \to \text{hadrons} \qquad (2)$$

was definitely not leading to a two-jet final state but was well consistent with models for three-jet final states[9]. Again, such final states were expected in QCD for the decay $\Upsilon \to 3$ gluons (Fig. 1c)[10].

A very intriguing question is whether one has already observed the pure glue states that are also expected in QCD. The indications for some of the mesonic states found in J/ψ decay to be glueballs (Fig. 1d) are indeed very suggestive[11]. A positive identification will have to rule out alternative interpretations as radially excited $q\bar{q}$ or as $q\bar{q}q\bar{q}$ systems, and will have to worry about mixing between gluonic and $q\bar{q}$ or $q\bar{q}q\bar{q}$ states.

Since the most unambiguous experimental tests for gluons come from three-jet states in e^+e^- annihilation, I will concentrate on these. What is the evidence that we are truly observing gluon jets?

It is instructive here to recall some history. The dominant two-jet structure of the process (1) was first seen at SPEAR at a center-of-mass energy of $W = 7.4$ GeV six years ago[12]. These jets were not well visible to the unaided eye. One needed an analysis in terms of the sphericity tensor and the angular distribution of the jet axis with respect to the incident e^+e^- beam, in order to convince oneself of the existence of these jets. Only at the higher energies of PETRA, at $W \approx 30$ GeV, this jet structure became immediately evident (Fig. 2). The interpretation of the two-jet final hadronic states as evolution products of primarily produced $q\bar{q}$ states rested on two cornerstones. The first was the total production cross section for these states (Fig. 3) [13]. For $q\bar{q}$ pair production it is predicted to be given by

$$R = \frac{\sigma_{tot}(e^+e^- \to \text{hadrons})}{\sigma^{(0)}_{tot}(e^+e^- \to \mu^+\mu^-)} \approx 3 \sum_{\text{flavours}} e_i^2 \left[1 + \frac{\alpha_s}{\pi} + o(\alpha_s^2)\right] \qquad (3)$$

where 3 is the color multiplicity of the quarks. While only very approximately true below $b\bar{b}$ threshold, this prediction was found to be very well verified by the high-energy data from PETRA and, recently, PEP. The second cornerstone was the angular distribution of the jet axis which agreed with the one expected for pointlike spin-$\frac{1}{2}$ particles[12]. A third one has been added only very recently from PETRA data, and it is the only one of these observations that relates to the specific characteristics of the evolution of the quarks into jets.

This is the observation of a long-range charge correlation between the two jets, shown to be not simply a consequence of overall charge conservation but to be of a dynamic nature characteristic for the evolution from oppositely charged primaries[14].

Let me now discuss the rarer class of three-jet events, an example of which is shown in Fig. 4. These events are seen at cm energies above about 25 GeV. One can select a kinematic region where each of the jets has an energy in the cm of at least, say, 6 GeV such that they are easily recognized and comparable to the jets in two-jet events at $W \gtrsim 12$ GeV. It is then not difficult to convince oneself that three separate jets indeed exist, and that they tend to lie in (or nearly in) a plane. This has been demonstrated clearly during the past two years in the PETRA experiments[7,15-17,32]. But what is the evidence that one of these jets comes from a gluon? Could it be a meson, a superposition of resonances, the product of a weak decay, or just a statistical fluctuation of the dominant two-jet configuration?

One of these possibilities can immediately be excluded, namely that it is a single meson. This is because the three jets, apart from at most quite subtle differences, look very much alike. This is true for such gross properties as the charged multiplicity $\langle n_{ch} \rangle$ at given energy E_{jet} of a jet[16], for the energy fraction E_{neut}/E_{jet} carried by neutrals[18], for the average transverse momentum $\langle p_T \rangle$ about the jet axis, and for the distribution of fractional longitudinal momentum x. As an example, Fig. 5 shows the result of a study by the JADE group[19] on a sample of $e^+e^- \to$ hadron events at $W = 30$ GeV which are planar but do not necessarily show three well resolved jets. One cuts the event into two halves by a plane perpendicular to the thrust axis $\hat{t}$ which is defined by maximizing the thrust

$$T = \max_{\hat{t}} \frac{\Sigma |\vec{p}_i \cdot \hat{t}|}{\Sigma p_i} \qquad (4)$$

One then selects the hadrons in that hemisphere which has the larger transverse momentum sum $\Sigma\, p_{Ti}$. These hadrons have a total invariant mass of typically ~12 GeV. In their common center-of-mass frame they are found to form a two-jet like configuration that looks very similar in shape to (2-jet) events $e^+e^- \to$ hadrons at $W = 12$ GeV, as shown by the close agreement of the thrust distributions for the two cases (Fig. 5).

As a consequence of this similarity in appearance of the three jets we have up to now not been able to identify the gluon among the three jets by its

characteristic hadronization properties. This is not surprising in view of what was mentioned before for quark jets, namely that establishing the simple property that the primary parton was charged, took 5 years after the discovery of the quark jets. To prove the existence of gluons we therefore are in a similar situation as we were until recently for quark jets, in that we have to rely on production properties like cross section, energy distributions, and angular correlations of the jets. These, fortunately, are uniquely predicted[8] in QCD; in lowest order they are identical to electromagnetic radiation except that α is replaced by $\frac{4}{3}\alpha_s$. We can thereby distinguish gluon radiation from other phenomena that might be suspected to be responsible for the observed event types in $e^+e^- \to$ hadrons. The question is whether these production properties have been non-trivially checked, or whether there are alternative possibilities for the interpretation of the observations. I will try to convince you that the data are adequate in precision such that they do not agree with just anything, but rather that the agreement with QCD is significant and constitutes a highly non-trivial test.

2. Energy flow in $e^+e^- \to$ hadrons

This section concerns one of the simplest and most straightforward measurements of the event shape, made by the MARK-J group[20]. Here, the energy of charged and neutral particles from reaction (1) is measured in a calorimeter surrounding the interaction region. Let the unit vector $\hat{k}_i$ describe the direction of the ith calorimeter element, and let E_i be the energy measured by it in a given event; we write $\vec{E}_i = E_i\hat{k}_i$. The thrust axis $\hat{t}$ is then given by maximizing the thrust

$$T = \max_{\hat{t}} \frac{\sum_i |\vec{E}_i \cdot \hat{t}|}{\sum_i E_i} = \frac{\sum |\vec{E}_{\parallel}|}{E_{tot}} \quad ; \tag{5}$$

the event plane is the plane normal to which the total energy flow $\Sigma|\vec{E}_{\perp out}|$ is a minimum, and the total energy flow in the event plane but perpendicular to $\hat{t}$ is denoted by $\Sigma|\vec{E}_{\perp in}|$. Planar events at $W \approx 35$ GeV are selected by requiring the 'oblateness' of the events defined by

$$O = \frac{\Sigma|\vec{E}_{\perp in}| - \Sigma|\vec{E}_{\perp out}|}{E_{tot}} \tag{6}$$

to be larger than 0.3. The azimuthal energy flow in the event plane, superimposing many events all with the thrust axis $\hat{t}$ pointing to the left and the

direction of maximum energy flow perpendicular to $\hat{t}$ pointing upwards, is shown in Fig. 6. The three-lobe pattern seen is partly an artifact of the construction of the energy flow diagram and does by itself not prove the existence of three distinct jets. Two-jet events or phase-space like events show a similar pattern (dashed and dashed-dotted curves). But it clearly appears that a QCD calculation for gluon bremsstrahlung in $o(\alpha_s)$ with $\alpha_s = 0.18$, using the diagrams of Fig. 1b, convoluted with a Monte Carlo simulation of hadronization[21] that also takes into account detector imperfections, describes the data better (solid curve) than either the phase space distribution or a $q\bar{q}$ two-jet model without gluons, regardless of whether the hadronization is assumed to produce a gaussian or an exponential $p_\perp$ distribution in the latter model. This conclusion does not rely on any assumptions about the mean p_T or the fragmentation functions in the $q\bar{q}$ models, since these parameters were independently fixed using the measured values of $\langle T \rangle$ and $\langle O \rangle$.

3. Energy-energy correlation in e^+e^- annihilation

A weakness of the energy flow analysis is that a meaningless pattern (the three lobes) pervades the analysis, such that the dynamic effects from gluon emission show up only as relatively minor variations to this built-in pattern. The significance of the conclusions from such an analysis relies strongly on the Monte Carlo simulation of the effects of hadronization and detector imperfections. One has tried to improve on this situation by more sophisticated analysis methods which will be discussed in the following.

One of these methodes uses the energy-energy correlation

$$\frac{1}{\sigma}\frac{d\Sigma_E(\Theta)}{d\Theta} = \lim_{\Delta\Theta\to 0}\frac{1}{\Delta\Theta}\sum_{j,k} x_j x_k \tag{7}$$

where

$$x_j = \frac{E_j}{E_{beam}} = \frac{E_j}{W/2} \tag{8}$$

is the fractional energy carried by the jth final state particle, and the sum runs over all those pairs j,k of an event whose momentum vectors span an angle Θ between them, falling into a given Θ bin of width $\Delta\Theta$. The result is then averaged over all events. Neglecting hadronization, i.e. considering q, $\bar{q}$ and g as the final state particles, this correlation has been calculated in perturbative QCD[22,23]. The result to $o(\alpha_s)$ is expected to be reliable for large angles Θ, say for $30^0 \lesssim \Theta \lesssim 150^0$, such that regions of collinear multi-gluon emission are avoided. In this angular region the perturbative contribution will be

$$\frac{1}{\sigma}\frac{d\Sigma_E^{pert}(\Theta)}{d\Theta} \propto \alpha_s(W^2) \propto \frac{1}{\ell n(W^2/\Lambda^2)} \quad . \tag{9}$$

For comparison with experimental results the perturbative calculation has to be convoluted with the non-perturbative hadronization effects. A simplified method to deal with hadronization[22] consists in approximating its effect by an additive contribution

$$\frac{1}{\sigma}\frac{d\Sigma_E^{NP}(\Theta)}{d\Theta} \propto \frac{1}{W} \tag{10}$$

which will vanish more strongly with increasing W than the perturbative contribution; however, in the W = 30 GeV region the two terms are still of similar magnitude. This is seen in Fig. 7 where the energy-energy correlation from the CELLO experiment is shown[24]. The agreement with the prediction adding (9) and (10) is good. The significance of this agreement is, however, difficult to judge due to the large size of the uncalculable non-perturbative contribution.

It is obviously preferable to consider quantities that are less affected by non-perturbative effects. Now in the simplest approximation the additive hadronization term (10) is expected to be symmetric under $\Theta \leftrightarrow \pi-\Theta$. On the other hand, the perturbative term (9) is asymmetric; this is easily understood from the fact that to inter-parton angles close to 180^0 both collinear and soft gluon emission contribute, while at $\Theta = 0$ only collinear emission can contribute. The forward-backward asymmetry

$$A(\Theta) = \frac{1}{\sigma}\left[\frac{d\Sigma_E}{d\Theta}(\pi-\Theta) - \frac{d\Sigma_E}{d\Theta}(\Theta)\right] \tag{11}$$

of the energy-energy correlation function is therefore expected to be largely free from the non-perturbative effects[22]. Results on $A(\Theta)$ from PLUTO[25], MARK-II[26] and CELLO[24] are shown in Fig. 8 and compared with an $O(\alpha_s)$ QCD prediction for $\alpha_s = 0.18$. One is tempted to conclude that the existence of this forward-backward asymmetry is a genuine manifestation of the presence of the perturbative QCD contribution in the energy-energy correlation function, and therefore of hard non-collinear gluon radiation.

Such a conclusion however would be premature since it rests on the simplifying assumption of angular symmetry of the hadronization effect and of a perfect detector. Among the effects that warrant careful evaluation are the following:

1) Detector imperfections. Energy flow or energy correlation measurements suffer uncertainties due to confusion between electrons, photons and hadrons in jets, due to escaping neutral particles, or to large fluctuations of energy deposit in total absorption calorimeters.

2) Radiative corrections. Radiation in the initial e^+e^- state in particular causes large changes of cross section and boosts the events into a moving frame, thus altering the angular correlations[27]. The effects are reduced by excluding events where the beam direction makes a small angle with the event plane, but they are never negligible.

3) Hadronization effects. The evolution of the partons to jets must at present be described by models. The relevant multiplicities, the $p_{||}$ and $p_{\perp}$ distributions (possibly involving long tails), the amount of resonance production, of baryon and strange particle production, and the effects of weak decays have to be considered.

Since all of these complications combine, they lead to correlated effects that can only be dealt with by Monte Carlo simulation. This is not to say that the effects are necessarily disturbingly large.

In the case of the energy-energy correlation, the PLUTO group has made a study of the aforementioned effects[25], using a QCD calculation incorporating hadronization in a Monte Carlo model[28,29]. It was found that the measured angular asymmetry $A(\Theta)$ is indeed dominated by the perturbative QCD contribution (9) at W = 30 GeV in the angular range $45^0 < \Theta < 90^0$, the total corrections from otner effects being on the 10 - 20 % level. Only at smaller energies and angles is $A(\Theta)$ substantially influenced by non-perturbative effects. Therefore, the agreement of the data on $A(\Theta)$ in Fig. 8 with perturbative QCD is indeed significant and can be taken as a strong indication of the presence of large-angle gluon bremsstrahlung.

4. W dependence of e^+e^- event shapes

It was mentioned before that the perturbative QCD contribution to the energy-energy correlation varies logarithmically with cm energy W, whereas the contribution from hadronization behaves like 1/W at high W. The same holds true for various other observable quantities that vanish for a pure $q\bar{q}$ final state and assume a value proportional to $\alpha_s(W^2)$ in leading-order QCD, such that the perturbative contribution to these observables is a measure of single hard gluon emission (Fig. 1b). The different W dependences of the perturbative and nonperturbative terms, logarithmic vs. 1/W, can be exploited to separate the two contributions. This has been done by the PLUTO collaboration who has data over a large W region both from DORIS and PETRA experiments[30].

The observables studied are i) thrust or rather <1-T>, ii) the energy-weighted jet broadness $\langle\sin^2\eta\rangle$, iii) the squared invariant mass of the wider of the two jets[31] (compare Fig. 5) divided by $s = W^2$, $\langle M_H^2/s\rangle$, and iv) the integral over the energy-energy correlation function in the large angle region $60^0 < \Theta < 120^0$. These quantities are shown in Fig. 9 as a function of W. The jet broadness is defined by[22]

$$\langle\sin^2\eta\rangle = \left\langle \frac{E_i}{W} \sin^2\delta_i \right\rangle \qquad (12)$$

where the average is taken over all final state particles of an event with energies E_i and angles δ_i with respect to the jet axis; η can be thought of as an energy-weighted jet opening angle.

The W dependences in Fig. 9 have been fitted with the sum of a $1/\ell n(W^2/\Lambda^2)$ and a 1/W term (cf. (9), (10)). The results of the fits are shown by the full curves and the contribution of the logarithmic (perturbative) term alone by the dashed curves in Fig. 9. The fits are very good and consistent with each other: the sizes of the perturbative QCD terms from the four independent fits give a consistent result for the value of α_s, namely $\alpha_s(W = 30\ \text{GeV}) = 0.18 \pm 0.02$. Although this analysis used the oversimplified assumption of additivity of the perturbative and nonperturbative contributions instead of properly convoluting the two, it is nevertheless remarkable that the W dependence exploited in this simplified fashion leads precisely to the same value for the strength of the gluon emission as the event shape and energy correlation measurements at fixed W. That QCD correctly describes the W dependence of the various event observables in $e^+e^- \to$ hadrons has, at only two energies but with a full hadronization Monte Carlo calculation,

also been quantitatively verified by the TASSO collaboration[16,32].

5. Jet angular correlations

All the observables discussed so far depend heavily on measurements of particle energies, which as mentioned before have relatively large uncertainties. Angles can in most storage ring detectors be measured much more precisely. Therefore, an approach more or less orthogonal to the ones described consists in using the particle energies only to divide the final state into "clusters" which can be associated with jets; once this is done, one uses only the directions of the jet axes.

To identify the jets as clusters of the particle four-momenta in phase space many different criteria and algorithms have been proposed and applied to the data. I mention triplicity[33], generalized sphericity[34], and more general cluster finding procedures like minimum spanning tree methods[35], hierarchical clustering algorithms[36], and others[37]. All of these methods have been found to reconstruct directions of jet axes to very good accuracy provided the energies and angular separations of the individual jets are not too small.

How large is "not too small"? Let us select a kinematic region for three-jet events by the requirement

$$x_1 < 0.9 \qquad (13)$$

where x_1, x_2, x_3 are the fractional energies ($x_j = E_j/E_{beam}$) of the three jets ordered such that

$$0 \le x_3 \le x_2 \le x_1 \le 1\ ; \qquad (14)$$

x_i is, for jet invariant masses M_{jet} small compared to W, identical with the thrust (4). From

$$x_1 + x_2 + x_3 = 2 \qquad (15)$$

it then follows that

$$0.2 < x_3 < 2/3 \qquad (16)$$

which means that the lowest energy jet has, for W = 35 GeV, a cm energy between 3.5 and 11.7 GeV. With $M_{jet}^2 \ll W^2$ the selection (13) further implies

$$M_{k\ell} > 11.1\ \text{GeV}, \quad \Theta_{k\ell} > 70^0 \qquad (17)$$

for the invariant mass of any pair of jets and the angular separation between them. This angular separation is larger than the angular width of the jets.

In the region so selected, the jet directions determined[34] from the data of the TASSO experiment were checked for consistency with energy-momentum conservation. The three directions are called momentum-nonconserving if $\Theta_{12} + \Theta_{23} + \Theta_{31} < 2\pi$, and are called energy-nonconserving if any of the three jet energies calculated (neglecting jet masses) from the $\Theta_{k\ell}$ is inconsistent with, i.e. smaller than, the observed jet energy. Allowing for the inherent resolution effects in the determination of the jet axes by a 1c-fit the fraction of energy-momentum violating three-jet events was found to be <1 % and entirely consistent with the fraction expected from fluctuations and radiative effects. This indicates that one suffers no major acceptance losses or other biases in the determination of the jet axes.

A further study of TASSO three-jet data was concerned with the stability of the jet directions with respect to a change of the jet-finding algorithm (triplicity[33] vs. generalized sphericity[34]) and with respect to including neutral or using charged particles only; the latter can usually be more precisely measured than the neutrals. While for individual events the various angles $\Theta_{k\ell}$ between the jet directions would undergo typical changes between $\pm 4^0$ and $\pm 8^0$, in no case was there a systematic bias exceeding 3^0. Equally small is the combined bias that results from the effects of resolution and acceptance of the detector, radiative corrections, and hadronization, which was determined by a Monte Carlo simulation.

We conclude from these investigations that in the TASSO detector the jet axes distributions can be consistently measured, at $W \approx 35$ GeV and in the kinematic region defined by $x_1 < 0.9$, to within a systematic uncertainty of only $\pm 2^0$.

The next question is whether the jet directions determined by such analyses agree with the momentum directions of the parent partons. A warning that such an assumption can be grossly wrong is given by the example[38] of the reaction

$$e^+e^- \to \pi^+\pi^- \qquad (18)$$

which has (because of helicity 1 in the initial state) a 'jet' angular distribution $1-\cos^2\Theta$, drastically different from the $1+\cos^2\Theta$ distribution of the parent $q\bar{q}$ state. The culprit is of course the angular momentum constraint in this exclusive reaction, with too few particles around to make a peaceful arrangement. Such final states are expected to get strongly suppressed when W increases so we need not be concerned.

However, things could be more subtle. The assumption jet direction = parent parton direction implies that each final state quark or gluon independently fragments in the overall cms. This is the physical basis of the Field-Feynman fragmentation model[28]. Alternatively in the color string model[39] each section of the string, extending from the q via the g to the $\bar{q}$, independently fragments in the rest frame of the separating colors. As these sections are boosted relative to the overall cms the jet directions, relative to which $\langle p_\perp^2 \rangle$ of the hadrons is minimum, will be slightly different from the parton directions. Indications for such a mechanism may have been observed[40] but the effect is subtle, predominantly involving slow fragments, and is negligible in our kinematic region of large angular separation between the jets.

Thus we are justified in identifying the measured jet axis angular correlations with parton angular correlations. We can also make a considerable simplification based on the fact that one finds very few genuine four-jet events. This is expected since in a $e^+e^- \to q\bar{q}gg$ transition one of the four partons almost always is either soft or closely collinear with one of the other partons. Consequently, if two-parton systems of invariant mass $M_{k\ell} < 6$ GeV are defined to lead to a single jet then one expects at $W \approx 35$ GeV a total four-jet rate of the order of only 2 % and a 4-jet/3-jet ratio of the order of 10 %. One therefore does not introduce a large error by using three-jet kinematics, as long as one is in a kinematic region that does not particularly enhance the contribution of four-jet events. This is confirmed by the consistency of the data with three-jet energy-momentum relationships as discussed above.

Instead of the angles $\Theta_{k\ell}$ between the jets we may then equally well use, in the approximation $M_{jet}^2 \ll W^2$, the fractional jet energies

$$x_j = \frac{E_j}{W/2} = \frac{2\sin\Theta_{k\ell}}{\sin\Theta_{12} + \sin\Theta_{23} + \sin\Theta_{31}} \qquad (19)$$

calculated from the measured angles. The correlation between the $\Theta_{k\ell}$ can then equivalently be described by the Dalitz plot of the three x_j. This approach to obtain the x_j through jet angular measurements leads to values that agree closely with the fractional energies of the parent partons. This has been ascertained with Monte Carlo-generated events for various different cluster finding procedures and different detectors. A result from MARK-II [35] which is typical also for others is shown in Fig. 10. The resolution in x_1 is 6 % and the systematic bias is seen to be very small; the TASSO analysis showed a bias of 1 %.

The jet Dalitz plot determined in this manner from the TASSO experiment at an average energy of W = 33 GeV is shown in Fig. 11. Such a plot contains the full dynamical information on the gluon bremsstrahlung process $e^+e^- \to q\bar{q}g$ if correlations with the beam and polarization directions are integrated over. Only 1/6 of the full Dalitz plot needs to be shown because of our inability to identify the gluon among the three jets which suggested the ordering (14) of the x_j. Collinear two-jet configurations lie along the base line of the plot, symmetric three-star configurations at the top corner. The proper three-jet kinematic region discussed before is the sub-triangle above the dotted line at $x_1 = 0.9$; it contains approximately 1/10 of all events.

The QCD prediction in $o(\alpha_s)$ for this plot is also shown in Fig. 11, assuming $\alpha_s = 0.17$. It was produced with a Monte Carlo simulation[29] to describe hadronization, and was passed through the detector and the same analysis procedure as the data. It agrees perfectly with the data. We note that the QCD distribution varies slowly over the whole three-jet region, such that smearing effects from finite resolution are small. For comparison we also show the Dalitz plot expected if 'gluons' were scalar[8]. It looks very similar to the other plots; only by a maximum likelihood analysis significant differences are revealed. However, the precise confidence level corresponding to a likelihood ratio is difficult to establish in the presence of finite resolution effects, and it is therefore safer to analyse one-dimensional projections of the Dalitz plot.

The projection on parton thrust x_1, normalized to σ_{tot}, is shown in Fig. 12 and is compared there with the QCD and scalar gluon predictions[8]. The agreement with QCD is impressive considering that the combined effects of hadronization, radiative corrections and detector imperfections are less than 30 % in this distribution. Therefore uncertainties in how to describe hadronization do not impair this analysis, and the measured x_1 distribution closely reflects the behaviour of the original partons. The comparison with QCD essentially involves then only the one parameter α_s which is determined to be 0.17 ± 0.02 from this analysis. The scalar gluon model, on the other hand, is seen not to fit the x_1 distribution well.

For a different projection of the jet Dalitz plot we consider the cosine of the Ellis-Karliner[41] angle (Fig. 13)

$$\cos\tilde{\theta} = \frac{x_2 - x_3}{x_1} = \frac{\sin\theta_{31} - \sin\theta_{12}}{\sin\theta_{23}} \,. \tag{20}$$

As the quark flips its spin in emission, for an emitted scalar parton the angular momentum change must be carried away as orbital angular momentum. This favours larger momenta and emission angles for the scalar parton than those typical for a QCD vector gluon, and consequently a smaller $\langle\cos\tilde{\theta}\rangle$. Unfortunately the observed $\cos\tilde{\theta}$ distribution will be strongly fudged by our inability to identify the gluon; instead of the third jet (x_3) being the gluon one calculates $\cos\tilde{\theta}$ with the third jet being the one of lowest energy. Due to the necessary ordering (14) of jet energies, moreover, the kinematic range of $\cos\tilde{\theta}$ depends on the value of x_1. These effects have to be taken into account in comparing the $\cos\tilde{\theta}$ distribution with QCD or with a scalar gluon model.

The distribution of $\cos\tilde{\theta}$ as determined in the TASSO experiment is shown in Fig. 14, selecting only the events in the three-jet region $x_1 < 0.9$. The comparison with vector gluon emission according to QCD involves no free parameter since α_s has already been fixed to fit the x_1 projection (as discussed in the last section); it is seen to fit the data perfectly (full curve). The particular virtue of the angle $\tilde{\theta}$ in discriminating against scalar 'gluons' can be seen from the two dashed curves in Fig. 14: this distribution, when determined via the $\theta_{k\ell}$, is hardly altered at all in going from the pure parton level to the observed distribution which involves hadronization, radiative corrections, and detector imperfections. For example the average value $\langle\cos\theta\rangle_{SCALAR}$ changes by only 1 % due to these effects. From this average over the three-jet region $x_1 < 0.9$ alone (which exploits only part of the available information but eliminates the sensitivity to the unknown coupling strength of scalar gluons[42]) we obtain

$$\begin{aligned} &\langle\cos\tilde{\theta}\rangle_{EXP} = 0.339 \pm 0.008 \\ \text{and}\quad &\langle\cos\tilde{\theta}\rangle_{EXP} - \langle\cos\tilde{\theta}\rangle_{QCD} = (2 \pm 8)\cdot 10^{-3} \\ &\langle\cos\tilde{\theta}\rangle_{EXP} - \langle\cos\tilde{\theta}\rangle_{SCALAR} = (41 \pm 8)\cdot 10^{-3} \,. \end{aligned} \tag{21}$$

This result was checked to be insensitive to the precise value of the x_1 cut[43]. It is important for this analysis that a three-jet identification

method was used that fits three axes to every event[34]; if two of the jets merge, the algorithm merges the jet axes but keeps the event in the sample, rather than assigning it to the different class of two-jet events and excluding it from the analysis, as some algorithms do. The latter procedure would have caused losses due to fluctuations in hadronization and to acceptance effects which would have necessitated large Monte Carlo corrections. We finally remark that $o(\alpha_s^2)$ QCD corrections to the shape of the $\cos\tilde{\Theta}$ distribution have been found to be quite small[44].

We conclude on the basis of these results from the TASSO experiment that scalar 'gluons' are inconsistent with the observed jet angular correlations at a 10^{-6} confidence level. This evidence from the $\cos\tilde{\Theta}$ distribution is further strenghtened by the x_1 distribution (Fig. 12). Earlier results from TASSO[42] and PLUTO[17] as well as preliminary results from MARK-II[26] also favour vector over scalar gluons.

6. Higher twist contributions, and models without gluons

We shall investigate next whether a part or all of the three-jet events could be due to the emission of a hard (large-p_T) meson or resonance instead of a gluon. Such processes (Fig. 15) are expected to be present in QCD at some level[45]. A specific model is the constituent interchange model (CIM). Dimensional counting at the emission vertex yields a factor $1/W^2$ relative to the leading pointlike (gluon emission) cross section. Thus, such higher twist contributions give

$$\langle p_T^2 \rangle_{HADRON} \sim \text{const} \quad \text{(independent of W)} \tag{22}$$

while gluon bremsstrahlung leads to

$$\langle p_T^2 \rangle_{GLUON} \sim \frac{\alpha_s(W^2)}{3\pi} W^2 \sim \frac{W^2}{\ell n(W^2/\Lambda^2)} \tag{23}$$

for the mean transverse momentum with respect to the thrust axis of the event.

Extending an earlier analysis by the PLUTO group[17], a comparison of the CIM model[46] with data from the TASSO experiment has been done assuming that the emitted hadron can be one of a whole spectrum of mesons that may decay into several pions; from the observed hadron multiplicity distribution of the three jets[16] it is already clear that single hard pion emission must be suppressed. The relevant quark-meson coupling strength is adjusted such that the model (without gluon bremsstrahlung) fits the observed p_T^2 distribution at W = 12 GeV (Fig. 16)[47]. To describe the p_T^2 distribution at W ≈ 33 GeV by this model however, a 4 times larger coupling constant (16 times larger cross

section contribution) would be necessary (Fig. 16). Moreover, even with such an enlarged coupling the model still falls short of describing the jet angular correlations at W = 33 GeV, as shown by the dashed-dotted curve in Fig. 12.

One estimates from these results that not more than 5 % of the cross section in the three-jet region at W ≈ 33 GeV can be attributed to the higher twist contribution.

The emission of a large-p_T meson M from a quark in the process $e^+e^- \to q\bar{q} \to q\bar{q}M$ (Fig. 15) may also involve a contribution with the same W dependence as the leading $e^+e^- \to q\bar{q}$ process but with an intrinsic p_T^{-4} tail of the hadron distribution. For comparison, gluon bremsstrahlung (which is point-like) has an intrinsic p_T^{-2} behaviour; on the other hand the most common assumption for hadronization is a gaussian p_T distribution, as used e.g. in the Field-Feynman model[28]. It turns out that while it is possible to adjust the p_T^{-4} tail of such a meson emission model so as to reasonably fit the TASSO p_T^2 distribution at a particular cm energy W, the strong W dependence of the p_T^2 distribution (shown in Fig. 16) is not correctly described. This is similar as with the higher twist contribution discussed before. The W dependence of the p_T^2 distributions appears to clearly call for a pointlike contribution. Moreover, subjecting Monte Carlo generated events from such a model to a three-jet analysis one obtains too few events with large angles between the three jets.

Incidentally the same conclusions on W dependence and inter-jet angles are reached for $e^+e^- \to q\bar{q}$ models in which the hadronization is given a long exponential tail. The inability of such a model to describe the observed energy flow in planar events was already remarked on in section 2.

While one cannot on the basis of such models 'explain the gluons away' one may ask how uncertain the measurement of the gluon coupling (i.e. of α_s) will become if a large-p_T meson emission process is assumed. A definitive answer is difficult to give but from confronting such models with TASSO data I estimate that α_s at W ≈ 30 GeV could decrease by something like 15 %.

A final remark concerns the viewpoint[48] that the entire tail in the p_T^2 distribution could be produced by the fragmentation of heavy quarks (c and b), which may impart a much larger intrinsic p_T^2 to their fragmentation products than light quarks do. A Monte Carlo simulation shows that in order to reproduce the observed p_T^2 distribution (Fig. 16) by such a model without gluons, one needs to assume rather large average transverse momenta in c and b quark

fragmentation. This has the consequence that planar events from this model will show a much too weak collimation around the three jet axes; in addition the fitted jet axes come out more collinear than in reality.

The purpose of the discussion in this section was to provide an understanding of how significant the agreement with QCD really is that we noted in the previous sections. We confronted the data with toy models like that for scalar gluons, or with actually expected but non-leading mechanisms like higher twist contributions, or with ad-hoc models specifically constructed to provide an alternate description not invoking gluons. The result is that the data indeed contain significant dynamical information to allow a discrimination. While alternatives to QCD gluon bremsstrahlung can usually be made to fit some of the relevant features of the data, no such model has been found or proposed (to my knowledge) that gives a reasonable description of all the major aspects of the available experimental information.

7. Next-to-leading order QCD corrections to $e^+e^- \to$ jets

It remains to convince ourselves that the good agreement between the three-jet data and the $o(\alpha_s)$ perturbative QCD calculation of gluon bremsstrahlung is not compromized by higher order contributions. The relevant diagrams (neglecting permutations) are shown in Fig. 17. They have been independently computed by different groups of theorists[49,50,51]. While their basic results for the matrix elements agree, different procedures are being used for the mutual cancelling of the singularities in the diagrams with four final state partons against those in the loop terms of the three-parton graphs, as well as for the treatment of the soft four-parton states. Consequently, the quantities calculated are different ones and it is not possible to directly compare the final results from all the second order calculations. Even the relative size of the $o(\alpha_s^2)$ corrections can, of course, differ significantly for the different types of observables.

Results from one of the calculations[49] have been supplemented by a calculation of hadronization effects and compared[52] to data from PETRA experiments; agreement is found for a strong coupling constant, at $W \approx 33$ GeV, of

$$\alpha_{\overline{MS}} = 0.13. \qquad (24)$$

The three-jet Sterman-Weinberg[53] type calculation yielded[50], on comparison with data at $W = 30$ GeV, the value

$$\alpha_{\overline{MS}} = 0.17 \ . \qquad (25)$$

In comparison with the value of $\alpha_s \approx 0.17$ extracted from the data using the $o(\alpha_s)$ calculation it should be remarked that in lowest order it is undefined which scale to use in the running coupling constant. It is often assumed that by evaluating α_s at the momentum transfer actually occurring in the gluon emission process, i.e. at

$$p^2 \approx (1 - x_1)W^2 \ , \qquad (26)$$

the higher order corrections are diminished. A value typical for the three-jet region at PETRA and PEP is $p^2 \approx 200$ GeV^2. The value of Λ in leading order will then be 110 MeV, and the corresponding value of α_s at a scale of $W \approx 33$ GeV is $\alpha_{LO} = 0.14$.

For the question of whether the $o(\alpha_s^2)$ calculations agree with the data the precise value of α_s is of lesser importance. What is relevant is that all three-jet quantities calculated to $o(\alpha_s^2)$ are found to have a nearly identical <u>shape</u> in $o(\alpha_s)$ and $o(\alpha_s^2)$. The example of the Ellis-Karliner angle was already mentioned. Our conclusion on the agreement of the three-jet data with perturbative QCD is therefore quite likely to hold to second order in α_s.

8. T decays into hadrons

After surveying the evidence for gluon jets produced in the e^+e^- continuum by color bremsstrahlung from quarks, we now shall briefly look at the self-annihilation of heavy $q\bar{q}$ bound states which should be an ideal source of gluon jets[10].

For vector states such as J/ψ or T the lowest order intermediate state involves three gluons (Fig. 1c) since one gluon is forbidden by color and two by angular momentum conservation. The three-gluon Dalitz plot distribution has been calculated to leading order in QCD[54]. Unfortunately the most probable configuration is one where two of the gluons share almost all of the available energy; such configurations will be difficult to distinguish from two-jet events. However, 38 % of the decays have angular separations of more than 80° between the directions of any two gluons. Such states must, in spite of hadronization smearing, look obviously different from two-jet events even at cm energies as low as W = 10 GeV, i.e. at the T mass. In general, however, there is considerable overlap of the three jets at this energy, making detailed analyses somewhat model-dependent.

It is therefore prudent to consider first a simple measure of the event shape that does not require the identification of three jet axes. We use the sphericity

$$S = \min_{\hat{s}} \frac{3}{2} \frac{\sum(\vec{p}_i \times \hat{s})^2}{\sum p_i^2} = \min \frac{3}{2} \frac{\sum p_{Ti}^2}{\sum p_i^2} \qquad (27)$$

which is 1 for ideally spherical and 0 for collinear states. Between W = 5 and 36 GeV the sphericity of e^+e^--produced hadronic final states (Fig.18) decreases monotonically with increasing W as the particles become increasingly collimated, with the exception of a sudden strong jump at resonance. The two-jet structure of the nearby continuum states disappears on resonance, and the events take an average sphericity of $\langle S \rangle \approx 0.4$, a value close to that expected for a phase space like distribution (with given hadron multiplicity).

The most detailed three-jet analysis of the final states from T decay has been carried out by the PLUTO collaboration [9]. The analysis concerns only the 'direct' hadronic decays, after subtraction of the contribution from the electromagnetic decay via one intermediate photon. The QCD predictions with which the data were compared, included the effects of detector acceptance, initial state radiative corrections,and hadronization. The gluon jets were assumed to fragment very much like the quark jets in the continuum.

It is found that the characteristic T event shape, which is very different from that in the nearby continuum, is reflected in many different distributions e.g. those of thrust T, of the angles $\Theta_{k\ell}$ between the jets, and of the fractional jet energies x_j calculated from the $\Theta_{k\ell}$ according to eq.(19). One of many examples is shown in Fig. 19 where the distribution of the angle Θ_{12}, the angle between the two most energetic jets, is plotted. It is compared with the three-gluon Monte Carlo prediction as well as with two versions of a uniform phase space distribution, one with only pseudoscalars (π,K) and the other with pseudoscalars and vector resonances in equal proportion. The lower part of Fig. 19 shows, for the sake of comparison, the corresponding distribution off resonance in comparison with a Field-Feynman $q\bar{q}$ Monte Carlo model. The T final states are seen to be strongly acollinear ($\langle\Theta_{12}\rangle$ very different from 180°); the precision of the data is good enough to distinguish the T decays clearly from the more collinear $q\bar{q}$ events on the one hand, as well as from phase space like Monte Carlo events on the other. The three-gluon QCD prediction describes the data well. The same has been found by PLUTO for all the other relevant distributions that were analyzed. Similar conclusions have been reached by the LENA group[55] and, recently, by the CLEO collaboration[56].

The significance of the agreement with QCD can be tested, as in the case of gluon bremsstrahlung, by asking whether a decay into three scalar 'gluons' could be ruled out. This is indeed the case. The Dalitz plot distribution for three scalar gluons favors almost collinear configurations of the two leading partons[57], yielding more two-jet like final states than observed. Another distribution sensitive to the vector/scalar nature of the three intermediate partons is the angular distribution of the most energetic jet (i.e. of the thrust axis) relative to the beam direction, shown in Fig. 20 from the LENA collaboration[55].

We remark that the inconsistency of the T decay states with two-jet $q\bar{q}$ states also proves that the gluons have color, since otherwise the decay $T \to g \to q\bar{q}$ via a single gluon into a pair of light quarks would be allowed[58].

A consistency check on the QCD notion of a lowest order $T \to 3g$ decay is provided by the total rate for this decay. Data from experiments both at DORIS and CESR give, after subtraction of the one-photon contribution, a value of $\Gamma_{dir} = (27 \pm 8)$ keV for the partial width corresponding to the 'direct' hadronic T decays. With this measurement the QCD calculation[59]

$$\frac{\Gamma(T \to 3g,\ 4g,\ q\bar{q}gg)}{\Gamma(T \to \mu^+\mu^-)} = \frac{10(\pi^2 - 9)}{81\pi}\,\frac{\alpha^3_{\overline{MS}}(m_T)}{\alpha^2}\,\frac{1}{e_b^2}\left[1 + 9.1\,\frac{\alpha_{\overline{MS}}(m_T)}{\pi}\right] \qquad (28)$$

yields $\alpha_{\overline{MS}}(M_T) = 0.14 \pm 0.01$ or $\Lambda_{\overline{MS}} \approx 120$ MeV, in agreement with other determinations of the strong coupling constant.

In summary, although the energies in T decay are too small to yield well-separated jets, it is clearly apparent that the final states are very different from the $q\bar{q}$ states in the nearby continuum. The QCD decay distribution folded with a hadronization model can describe the data while a three-scalar-parton decay will not do. All available evidence clearly points towards the existence of the T → 3 gluons decay process.

9. Conclusion

QCD, the candidate theory of the strong interactions, has been remarkably successful in the past years. Many of its outstanding predictions, most notably the scaling violations in nucleon structure functions, were confirmed be experiment. A major triumph of QCD was the observation of three-jet events in high energy e^+e^- annihilation into hadrons. Such events were predicted to occur as a result of hard gluon bremsstrahlung. They exhibit the parton properties of the color field, manifesting themselves as jets in complete analogy with the quarks and allowing to directly verify the vector nature of the radiated field quanta. Attempts for an alternative explanation of the phenomena by various models have not been successful. The corollary that gluons as partons should be triple-produced in T decay has also been tested and provides direct evidence for the gluon to be colored.

Taking all the evidence together we can now consider it well verified that whenever quarks are treated violently, be it by sudden creation as in e^+e^-, sudden annihilation as in T decay, or by a hard kick from a scattering lepton, they react by spilling out colored glue that we can catch in our detectors. Wondering into what the glue then evolves will surely keep us busy for some time.

Acknowledgement

I wish to thank the Weizmann Institute of Science where much of the work reported in Sections 5 and 6 was done, and in particular Profs. G. Mikenberg and U. Smilansky, for their kind hospitality and a very pleasant stay. I am particularly indebted to U. Karshon, G. Rudolph, G. Wolf and S.L. Wu for a fruitful collaboration. Finally it is a pleasure to thank Prof. C.A. Heusch who invited me to this very stimulating conference.

References

1. For a review see J.I. Friedman and H.W. Kendall, Ann.Rev.Nuc.Sci. 22, 203 (1972).

2. R.P. Feynman, Photon-Hadron Interactions (Benjamin, Reading, Mass. 1972), p. 152;
D.H. Perkins, Proc. 16th Int. Conf. on High Energy Physics, Chicago-Batavia 1972 (NAL, Batavia 1972), Vol.4, p. 189.

3. D.J. Gross and F. Wilczek, Phys.Rev. D8, 3633 (1973); D9, 980 (1974);
H. Georgi and H.D. Politzer, Phys.Rev. D9, 416 (1973);
J.B. Kogut and L. Susskind, Phys.Rev. D9, 697 (1974); 3391 (1974).

4. For recent reviews see D.H. Perkins, Acta Physica Polonica B11, 39 (1980);
J. Ellis, Proc. 1979 Int. Symp. on Lepton and Photon Interactions (FNAL, Batavia, Illinois), p. 412;
A.J. Buras, Rev.Mod.Phys. 52, 199 (1980);
E. Reya, Phys.Reports 69, 195 (1981);
G. Altarelli, Phys.Reports to be published.

5. J. Drees, Proc. 1981 Int. Symp. on Lepton and Photon Interactions at High Energies, Bonn (1981);
J.J. Aubert et al., Phys.Lett. 100B, 433 (1981);
J. Gayler, Proc. Int. Conf. on High Energy Physics (Lisbon 1981), and Preprint DESY 81-063 (1981);
H.C. Ballagh et al., Phys.Rev.Lett. 47, 556 (1981).

6. R. Brandelik et al. (TASSO collaboration), Phys.Lett. 86B, 243 (1979);
D.P. Barber et al. (MARK-J collaboration), Phys.Rev.Lett. 43, 830 (1979);
C. Berger et al. (PLUTO collaboration), Phys.Lett. 86B, 418 (1979);
W. Bartel et al. (JADE collaboration), Phys.Lett. 91B, 142 (1980).

7. A.M. Polyakov, Proc. 7th Int. Symp. on Lepton and Photon Interactions at High Energies (Stanford 1975), p. 855.

8. J. Ellis, M.K. Gaillard, and G.G. Ross, Nucl.Phys. B111, 253 (1976).
For a review on gluons in QCD see J. Ellis, Comm.Nucl.Part.Phys. 9, 153 (1980).

9. C. Berger et al. (PLUTO collaboration), Z. Phys. C (Particles and Fields) 8, 101 (1981).

10. T. Appelquist and H.D. Politzer, Phys.Rev.Lett. 34, 43 (1975); Phys.Rev. D12, 1404 (1975).

11. D. Scharre, Proc. 1981 Int. Symp. on Lepton and Photon Interactions at High Energies (Bonn 1981).

12. G.G. Hanson et al., Phys.Rev.Lett. 35, 1609 (1975);
R.F. Schwitters et al., Phys.Rev.Lett. 35, 1320 (1975).

13. For a recent compilation, see R. Felst, 1981 Int. Symp. on Lepton and Photon Interactions at High Energies (Bonn 1981), and also ref. 32.

14. R. Brandelik et al. (TASSO collaboration), Phys.Lett. 100B, 357 (1981).

15. D.P. Barber et al. (MARK-J collaboration), Phys.Reports 63, 337 (1980);
Phys.Lett. 89B, 139 (1979).

16. R. Brandelik et al. (TASSO collaboration), Phys.Lett. 94B, 437 (1980).

17. C. Berger et al. (PLUTO collaboration), Phys.Lett. 97B, 459 (1980).

18. W. Bartel et al., (JADE collaboration), Z. Physik C (Particles and Fields) 9, 315 (1981).

19. A. Petersen (JADE collaboration), Proc. 15th Rencontre de Moriond (Les Arcs 1980); DESY report 80/46 (1980);
W. Bartel et al., Phys.Lett. 91B, 142 (1980).

20. D.P. Barber et al (MARK-J collaboration), MIT-LNS report No. 115 (1981).

21. A. Ali, E. Pietarinen, G. Kramer, and J. Willrodt, Phys.Lett. 93B, 155 (1980). A similar approach to hadronization, ref.29, has also been used.

22. C.L. Basham, L.S. Brown, S.D. Ellis, and S.T. Love, Phys.Rev.Lett. 41, 1585 (1978); Phys.Rev. D17, 2298 (1978); Phys.Rev. D19, 2018 (1979).

23. G.C. Fox and S. Wolfram, Nucl.Phys. B149, 413 (1979).

24. D. Fournier (CELLO collaboration), Proc. of the 1981 Int. Symp. on Lepton and Photon Interactions at High Energies (Bonn 1981).

25. C. Berger et al., (PLUTO collaboration), Phys.Lett. 99B, 292 (1981).

26. R. Hollebeek (MARK-II collaboration), Proc. 1981 Int. Symp. on Lepton and Photon Interactions at High Energies (Bonn 1981).

27. F.A. Berends and R. Kleiss, DESY reports 80/66, 80/73 (1980), to be published.

28. R.D. Field and R.P. Feynman, Nucl.Phys. B136, 1 (1978).

29. P. Hoyer et al.,Nucl.Phys. B161, 349 (1979); T. Meyer, unpublished.

30. C. Berger et al. (PLUTO collaboration), preprint DESY 81-054 (1981).

31. L. Clavelli and D. Wyler, preprint Univ. Bonn HE-81-3

Figure Captions

Fig. 1 a) Emission of (undetected) gluons by quarks in the nucleon, leading to scaling violation in the nucleon structure functions

b) Leading diagram and lowest-order QCD radiative correction (gluon bremsstrahlung) for $e^+e^- \to$ hadrons, leading to two- and three-jet events

c) Self-annihilation of $b\bar{b}$ quark pairs in the T bound state, producing hadrons via three intermediate gluons

d) Radiative J/ψ decays producing color-singlet gluon pairs, and possibly glueball states.

Fig. 2 A typical two-jet event observed at PETRA. The view is along the e^+e^- beam axis. Low-momentum particles may emerge at large angles to the jet axis, as shown by the two tracks going towards the upper right corner. Note that the neutrals whose energy is measured by the calorimeter surrounding the tracking region, are as well collimated into jets as the charged particles are.

Fig. 3 The ratio R of the total cross section for e^+e^- annihilation into hadrons to the lowest-order muon pair cross section $\sigma^{(o)}_{tot}(e^+e^- \to \mu^+\mu^-) = 4\pi\alpha^2/3W^2$.

Fig. 4 A three-jet event observed at PETRA. The view is along the beam axis into the interior of the JADE detector, shown in perspective: the outer radius is the nearby edge, the inner radius the opposite distant edge of the cylindrical tracking region. The tracking region has a diameter of 1.6 m and a length of 2.4 m. On the inner surface of the shower counter the actual segmentation is indicated; those segments in which energy has been deposited, are marked in black.

Fig. 5 On the top, a procedure of studying the structure of the wide jet in planar events from the reaction $e^+e^- \to$ hadrons is shown. The lower part shows the comparison of event shapes measured by thrust (T = 1/2 for spherical, T = 1 for collinear states), i) for the wide jet (transformed to its rest system) of planar events at 30 GeV, and ii) for complete events at 12 GeV (nearly all being 2-jet events). From ref. 19.

Fig. 6 Energy flow observed for planar events of the reaction $e^+e^- \to$ hadrons, as a function of the azimuthal angle in the event plane relative to the thrust axis $\hat{t}$, from ref. 20. The curves show fits by i) a QCD calculation (full curve) with $\alpha_s = 0.18$, ii) a two-jet $q\bar{q}$ model with a Gaussian (dashed) or exponential (dotted) p_T distribution, iii) a pure phase space distribution (dashed-dotted curve).

Fig. 7 Angular dependence of the energy-energy correlation function in the reaction $e^+e^- \to$ hadrons, corrected for detector acceptance (ref. 24). The curves show the parton-level $o(\alpha_s)$ QCD prediction (dashed) and the effect of adding a hadronization contribution (solid curve, ref. 22).

Fig. 8 Forward-backward asymmetry of the energy-energy correlation function in the reaction $e^+e^- \to$ hadrons, from refs. 24, 25, 26. The curve indicates the QCD prediction to $o(\alpha_s)$ with $\alpha_s = 0.18$; precise predictions (ref.25) involve small experiment-dependent corrections.

Fig. 9 W-dependences of average thrust, energy-weighted jet broadness, squared invariant mass of the "heavy" jet, and of the integral over the wide-angle part of the energy-energy correlation function in the reaction $e^+e^- \to$ hadrons (from ref. 30). The curves show the results of fits by a two-term formula $a/\ell n(W^2/\Lambda^2) + b/W$; the first term describes the logarithmic W-dependence of the $o(\alpha_s)$ QCD contributions (on the parton level), the second term approximates hadronization effects. From the size of the perturbative QCD terms one extracts $\alpha_s = 0.18 \pm 0.02$.

Fig.10 Ratio of reconstructed to generated parton thrust x_1 for Monte Carlo simulated events of the reaction $e^+e^- \to$ hadrons at $W \approx 30$ GeV (from ref. 35).

Fig.11 Dalitz plot of the three reconstructed jet energies for the reaction $e^+e^- \to$ hadrons at $\langle W \rangle = 33$ GeV, from the TASSO experiment (top plot). For comparison, the QCD prediction to $o(\alpha_s)$ with $\alpha_s = 0.17$ and the prediction for scalar gluon radiation are shown using Monte Carlo simulations with the same number of events (middle and bottom plots). The scalar coupling is given by $\tilde{\alpha}_s = 1.6$, choosen to optimize overall agreement with a number of event variables (ref. 42).

32. For a review see P. Söding and G. Wolf, Ann.Rev.Nucl.Part. Sci. 31, 231 (1981).

33. S. Brandt and H.D. Dahmen, Z. Physik C (Particles and Fields) 1, 61 (1979).

34. S.L. Wu and G. Zobernig, Z. Physik C (Particles and Fields) 2, 107 (1979); S.L. Wu, Z. Physik C (Particles and Fields) 9, 329 (1981).

35. J. Dorfan, Z. Physik C (Particles and Fields) 7, 349 (1981); and private communication.

36. K. Lanius, H.E. Roloff and H. Schiller, Z. Physik C (Particles and Fields) 8, 251 (1981.

37. H.J. Daum, H. Meyer, and H. Bürger, Z. Physik C (Particles and Fields) 8, 167 (1981).

38. K.G. Tabrizi and D.M. Webber, Nucl.Phys. B181, 301 (1981).

39. B. Andersson, G. Gustafson, and T. Sjöstrand, Phys.Lett. 94B, 211 (1980), and earlier references given there.

40. W. Bartel et al. (JADE collaboration), Phys.Lett. 101B, 129 (1981).

41. J. Ellis and I. Karliner, Nucl.Phys. B148, 141 (1979).

42. See the detailed discussion in R. Brandelik et al. (TASSO collaboration), Phys.Lett. 97B, 453 (1980).

43. Obviously for an x_1 cut much lower than 0.9 the diminishing statistics and kinematic range of $\cos\tilde{\Theta}$ will decrease the significance of the scalar/vector discrimination, while with a cut close to or exceeding 0.95 one runs the risk of getting too close to the two-jet region (see Fig. 11) and therefore to get sensitive to hadronization effects.

44. Z. Kunszt, private communication

45. J.F. Gunion, The Case for Higher Twist, III. Int. Warsaw Symp. on El. Part. Physics (1980); UC Davis preprint (1981).

46. T.A. De Grand, Y.J. Ng, and S.H. Tye, Phys.Rev. D16, 3251 (1977).

47. The quark-meson coupling needed for the fit at W = 12 GeV agrees with the one extracted from other experiments using the constituent interchange model in Ref. 46; in their notation it is given by $(g/4\pi)^2_{\text{effective}} = 200\ \text{GeV}^2$.

48. C.K. Chen, Purdue Univ. preprints (1980, 1981); Phys.Rev. D23, 712 (1981).

49. R.K. Ellis, D.A. Ross, and A.E. Terrano, Phys.Rev.Lett. 45, 1226 (1980); Nucl.Phys. B178, 421 (1981);
D.A. Ross, Nucl.Phys. B188, 109 (1981);
Z. Kunszt, Phys.Lett. 99B, 429 (1981), and preprint TH-3141-CERN (1981).

50. K. Fabricius, I. Schmitt, G. Schierholz, and G. Kramer, Phys.Lett. 97B, 431 (1980); preprint DESY 81-035 (1981); see also earlier references quoted there.

51. J.A.M. Vermaseren, K.J.F. Gaemers, and S.J. Oldham, Nucl.Phys. B187, 301 (1981);
S. Sharpe, preprint LBL-13018 (1981).

52. A. Ali, preprint DESY 81-059 (1981).

53. G. Sterman and S. Weinberg, Phys.Rev.Lett. 39, 1436 (1977).

54. K. Koller and T.F. Walsh, Phys.Lett. 72B, 227 (1977), (E: 73B, 504); Nucl.Phys. B140, 449 (1978);
S.J. Brodsky, T.A. De Grand, R.R. Horgan, and D.G. Coyne, Phys.Lett. 73B, 203 (1978);
H. Fritzsch and K.H. Streng, Phys.Lett. 74B, 90 (1978);
A. deRujula et al., Nucl.Phys. B138, 387 (1978);
K.Koller, H.Krasemann, and T.F. Walsh, Z. Physik C (Particles and Fields) 1, 71 (1979).

55. B. Niczyporuk et al. (LENA collaboration), Z. Physik C (Particles and Fields) 9, 1 (1981).

56. D. Schamberger (Cornell), Proc. 1981 Int. Symp. on Lepton and Photon Interactions at High Energies (Bonn 1981); A. Silverman, ibid.

57. K. Koller and H. Krasemann, Phys.Lett. 88B, 119 (1979).

58. T.F. Walsh and P.M. Zerwas, Phys.Lett. 93B, 53 (1980).

59. P.B. Mackenzie and G.P. Lepage, preprint CLNS/81-498 (1981).

Fig. 12 Distribution of the maximum reconstructed jet energy x_1 (= parton thrust for three-jet events) in the reaction e^+e^- → hadrons at $\langle W \rangle$ = 33 GeV, from the TASSO experiment. The full curve shows the QCD prediction to $o(\alpha_s)$ with $\alpha_s = 0.17$, the dashed curve the prediction for scalar gluons (with the coupling $\tilde{\alpha}_s = 1.6$ optimized to furnish the best overall description of a number of event variables (ref. 42)). The dashed-dotted curve is the prediction from the constituent interchange model with a scaled-up coupling constant such as to fit the p_T^2 distribution at the same energy (see Fig. 16 and the associated discussion).

Fig. 13 a) Momenta and angles of a three-parton state in the cm frame

b) The same state transformed to the rest frame of partons 2 and 3

Fig. 14 Observed distribution of the Ellis-Karliner variable $\cos\tilde{\Theta}$ (defined in eq.(20)), for events in the three-jet region defined by parton thrust $x_1 < 0.9$ for the reaction e^+e^- → hadrons at $\langle W \rangle$ = 33 GeV (from the TASSO experiment). The full curve shows the QCD prediction to $o(\alpha_s)$ with $\alpha_s = 0.17$ (vector gluons), the dashed-dotted curve the prediction for scalar gluons. (The latter is normalized to the observed distribution in this plot; this corresponds to a coupling $\tilde{\alpha}_s = 1.1$). The dashed curve shows the scalar gluon prediction on the parton level, i.e. before correction for hadronization, radiative effects, and detector imperfections.

Fig. 15 Diagrams for large-p_T meson production in the process $e^+e^- \to q\bar{q}M$.

Fig. 16 Distribution of the square of the transverse momentum of charged particles with respect to the jet axis in the reaction e^+e^- → hadrons at different cm energies W (from the TASSO experiment, see ref. 32). The dashed curve shows the prediction from the constituent interchange model (ref. 46) at W = 12 GeV; the dashed-dotted curve is for W = 33 GeV with a scaled-up $q\bar{q}M$ coupling so as to approximately fit the data.

Fig. 17 QCD diagrams relevant for e^+e^- → hadrons to $o(\alpha_s^2)$.

Fig. 18 The average sphericity in e^+e^- → hadrons as measured by the JADE, PLUTO and TASSO experiments as a function of cm energy W.

Fig. 19 Distribution of the reconstructed angle Θ_{12} between the two most energetic jets, for the direct decay Υ → hadrons and for off-resonance e^+e^- continuum events (from ref. 9). The curves show a three gluon QCD calculation, a phase-space Monte Carlo model for production of only pseudoscalar or of pseudoscalar and vector mesons, and a Field-Feynman $e^+e^- \to q\bar{q}$ calculation.

Fig. 20 Angular distribution of the thrust axis for off-resonance e^+e^- continuum events and for direct hadronic Υ decays. The curves for Υ decays show the predictions for decays into three vector or scalar gluons. (From ref. 55).

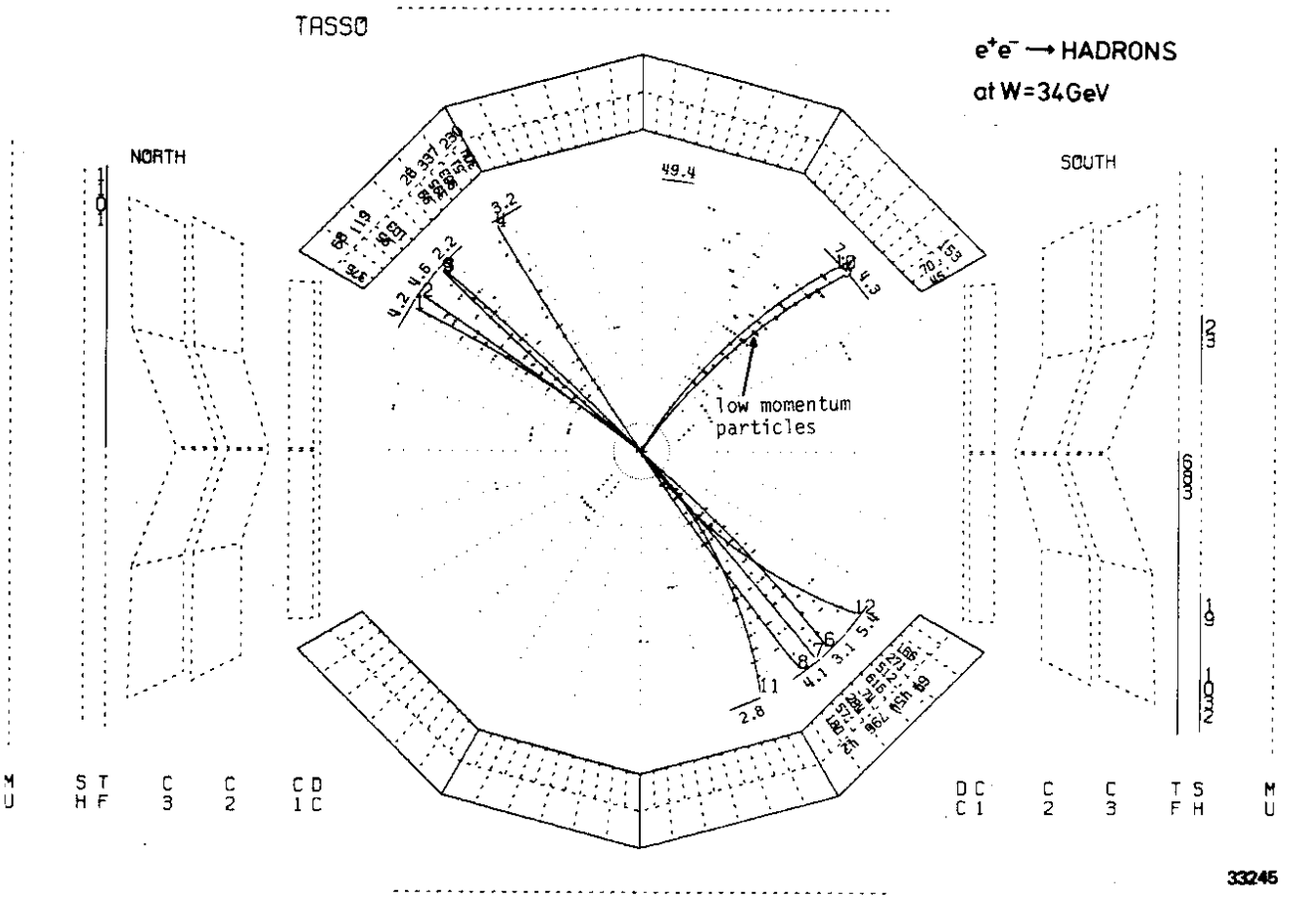
TASSO
e⁺e⁻ → HADRONS
at W=34GeV
NORTH
SOUTH
low momentum
particles
49.4
33245

Fig. 2

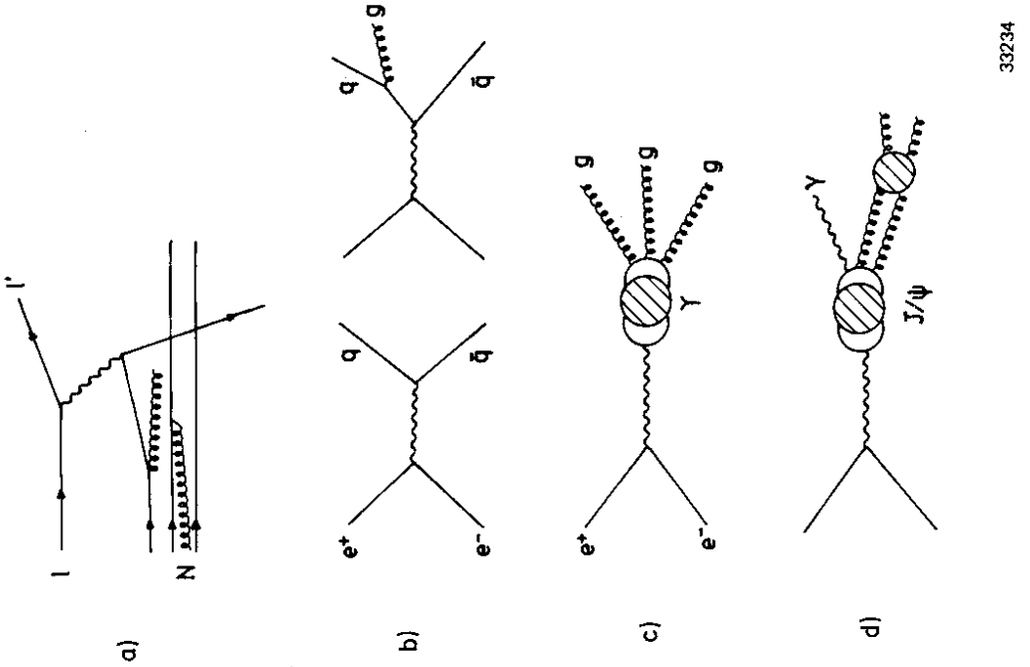
l'
l
N
q
q̄
g
e⁺
e⁻
γ
J/ψ
a)
b)
c)
d)
33234

Fig. 1

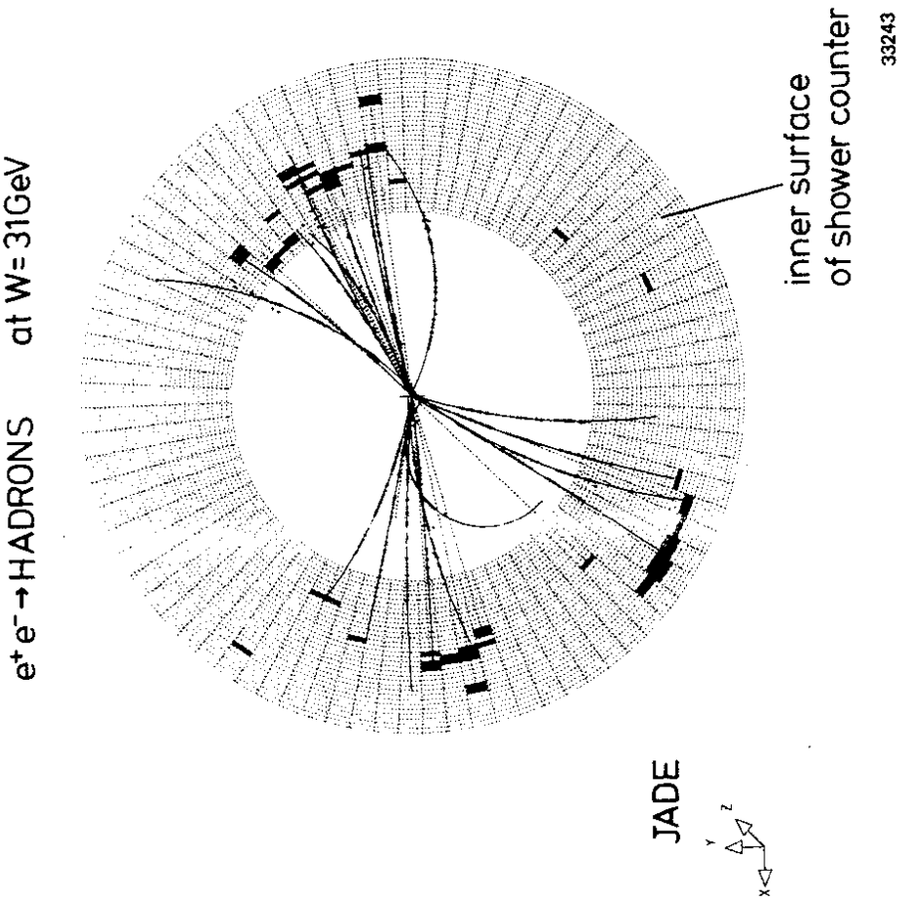
e⁺e⁻→HADRONS at W=31GeV
inner surface of shower counter
33243
JADE

Fig. 4

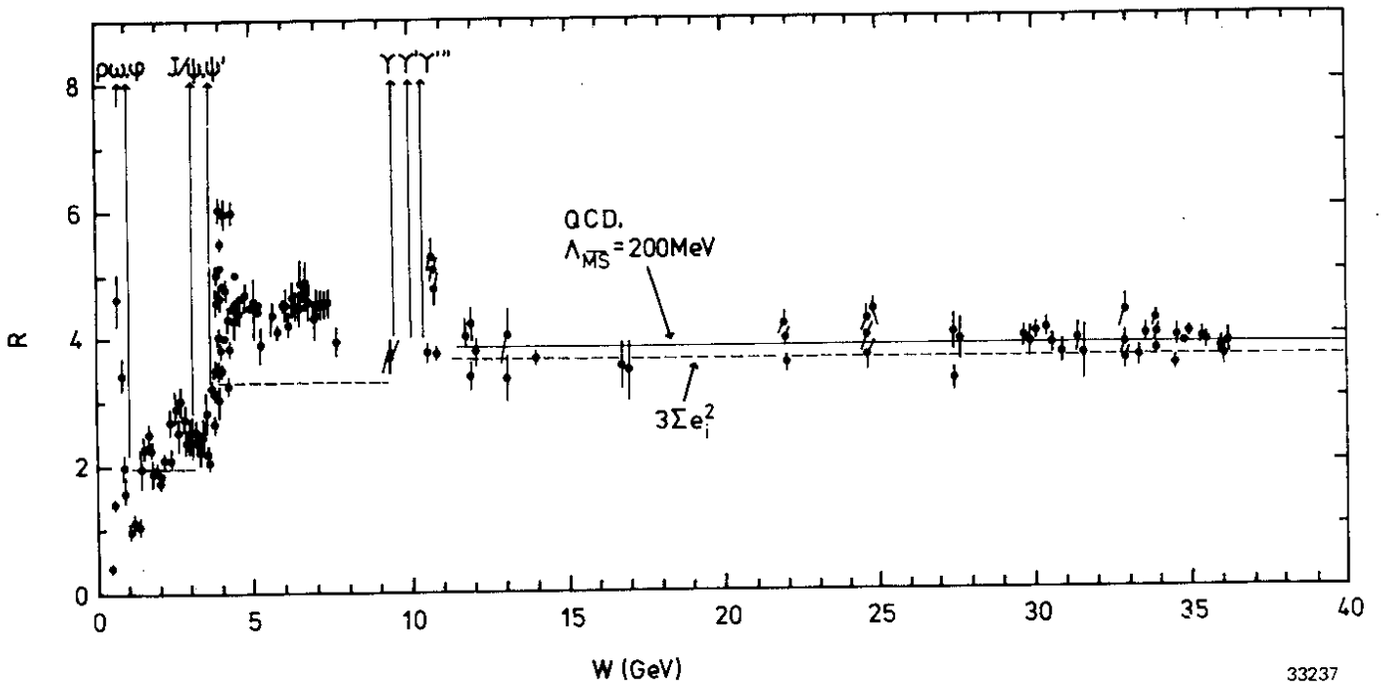
ρ ω φ
J/ψ ψ'
ϒ ϒ' ϒ''
QCD.
$\Lambda_{\overline{MS}}$ = 200MeV
$3\Sigma e_i^2$
R
W (GeV)
0
2
4
6
8
0
5
10
15
20
25
30
35
40
33237

Fig. 3

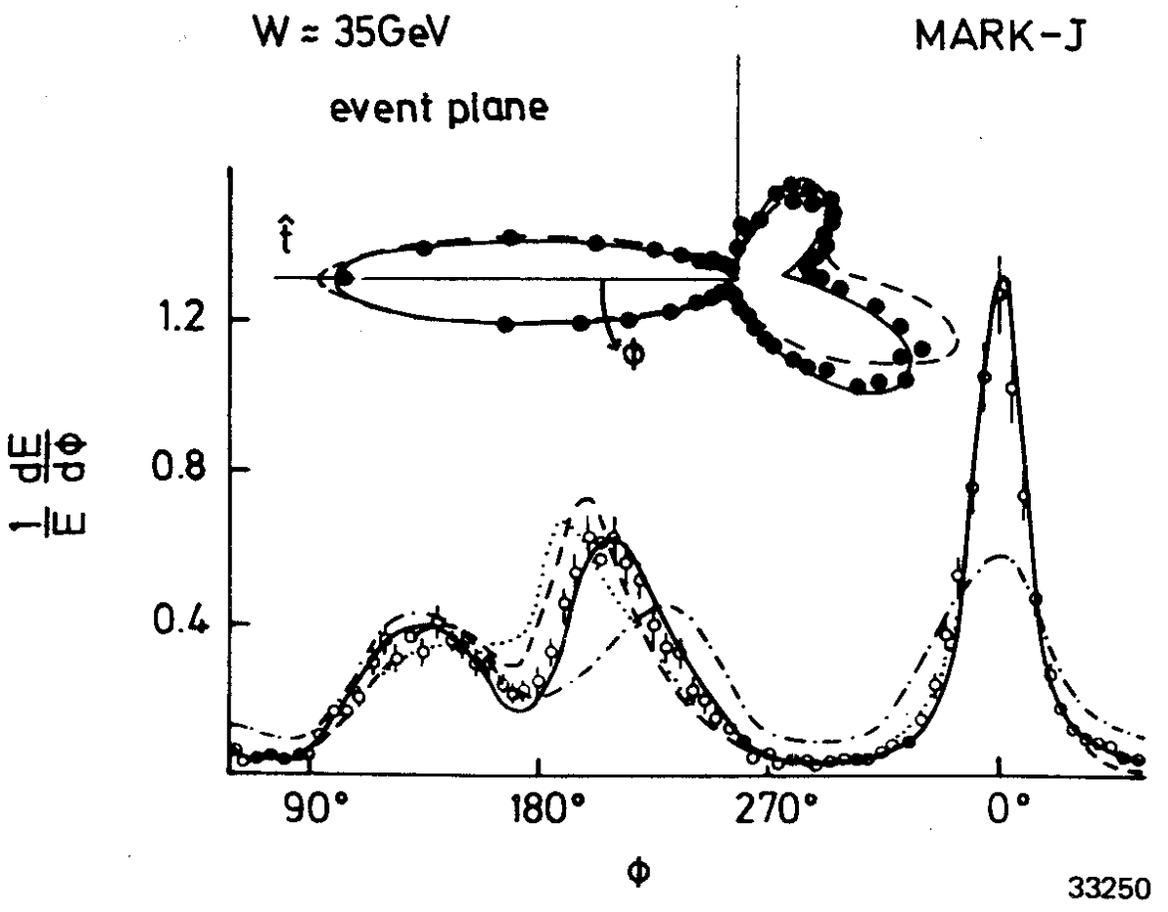
W ≈ 35GeV
MARK-J
event plane
t̂
Φ
1.2
0.8
0.4
1/E dE/dΦ
90°
180°
270°
0°
Φ
33250

Fig. 6

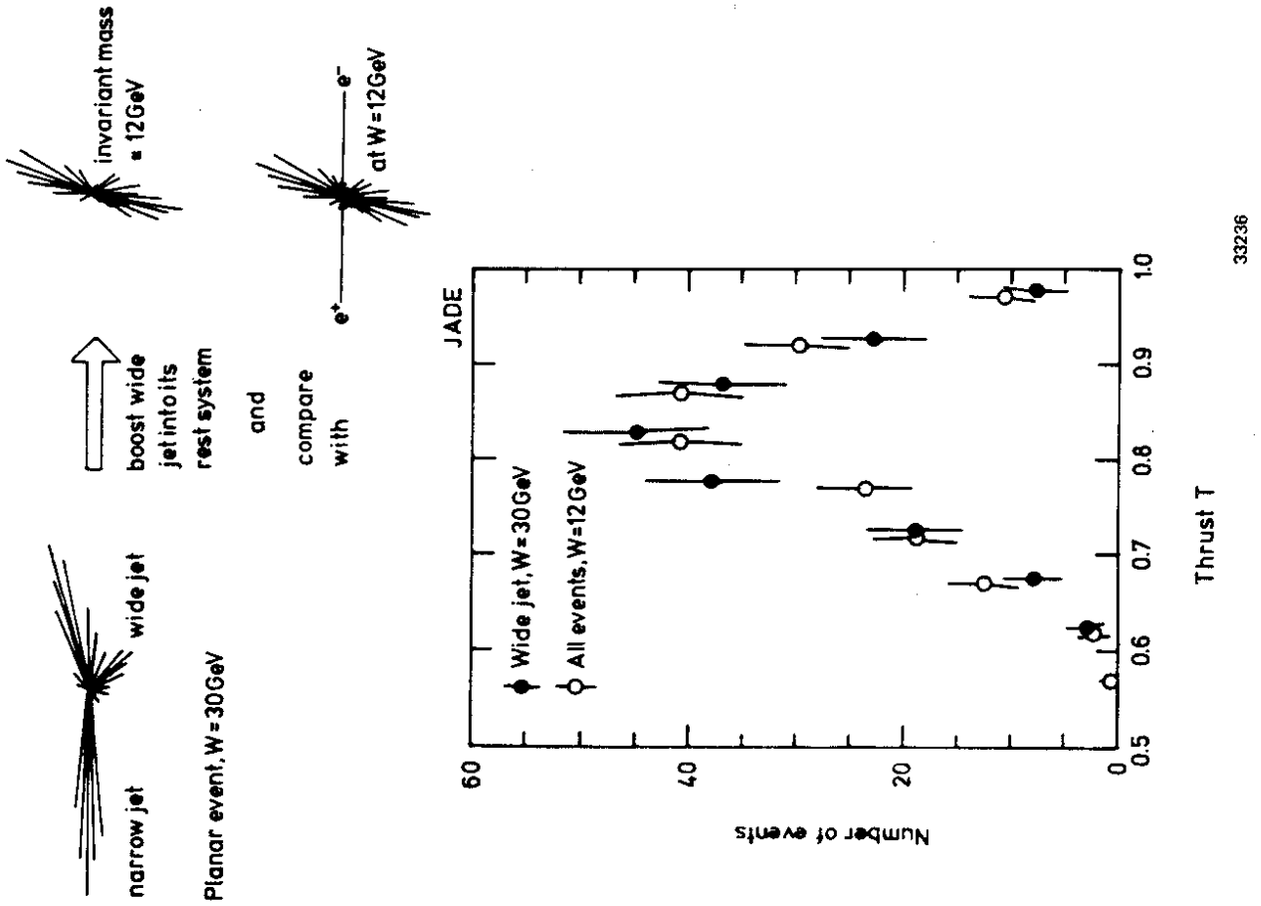
invariant mass = 12GeV
boost wide jet into its rest system
and
compare with
e⁻
e⁺
at W=12GeV
wide jet
narrow jet
Planar event, W=30GeV
JADE
Wide jet, W=30GeV
All events, W=12GeV
Number of events
Thrust T
60
40
20
0
0.5
0.6
0.7
0.8
0.9
1.0
33236

Fig. 5

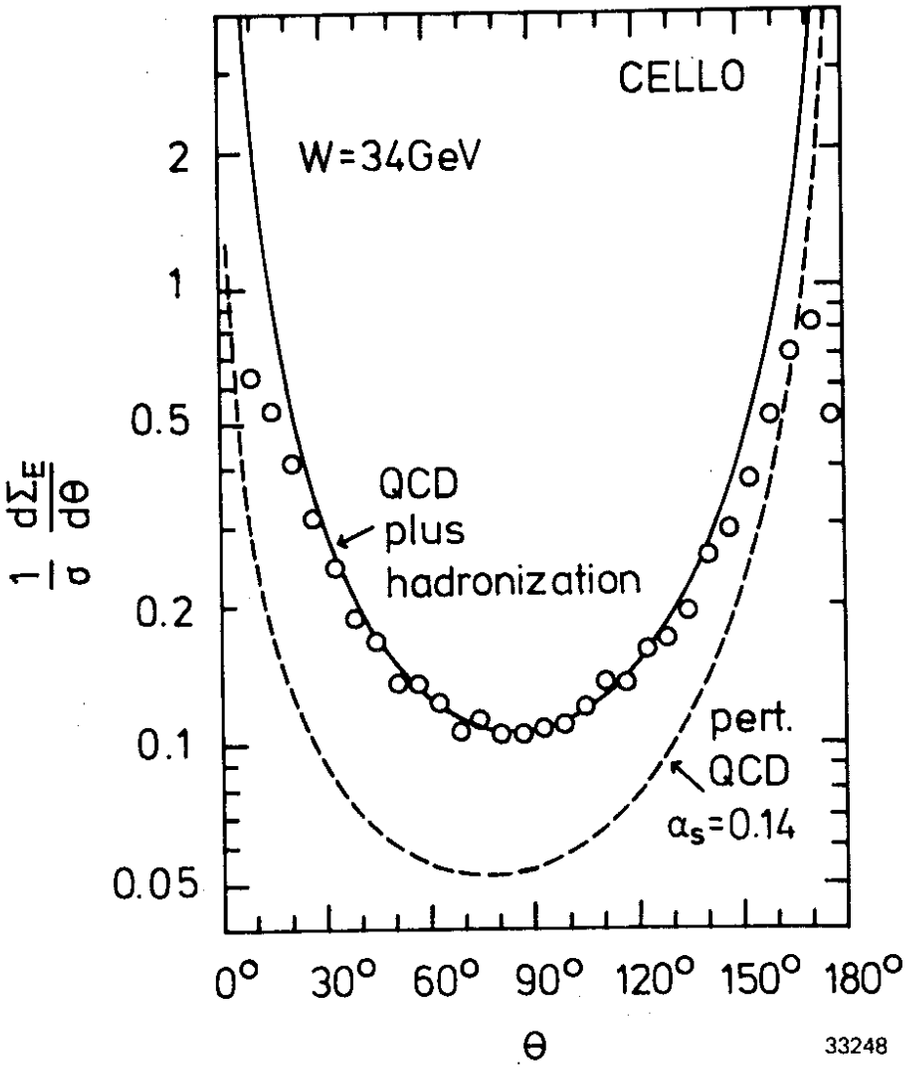
CELLO
W=34GeV
QCD
plus
hadronization
pert.
QCD
α_s=0.14
$\frac{1}{\sigma}\frac{d\Sigma_E}{d\theta}$
2
1
0.5
0.2
0.1
0.05
0°
30°
60°
90°
120°
150°
180°
θ
33248

Fig. 7

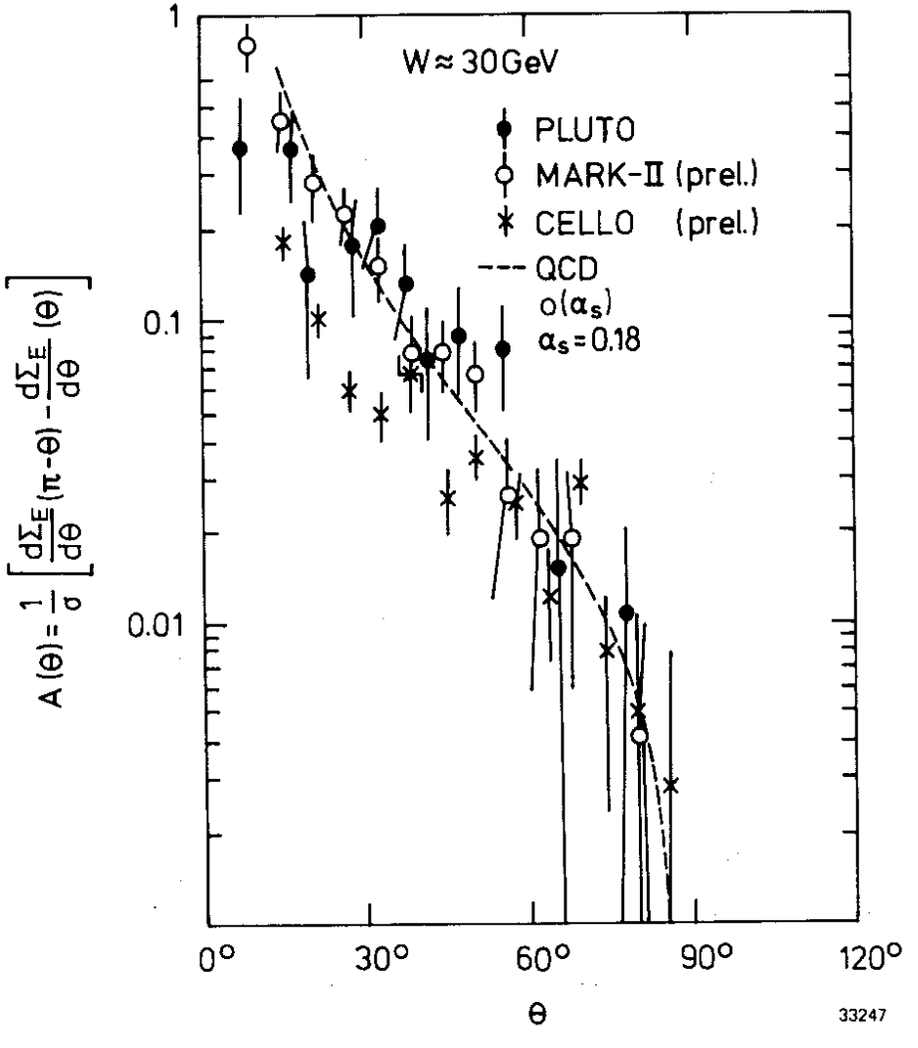
W≈30GeV
PLUTO
MARK-II (prel.)
CELLO (prel.)
QCD
$o(\alpha_s)$
α_s=0.18
$A(\theta)=\frac{1}{\sigma}\left[\frac{d\Sigma_E}{d\theta}(\pi-\theta)-\frac{d\Sigma_E}{d\theta}(\theta)\right]$
1
0.1
0.01
0°
30°
60°
90°
120°
θ
33247

Fig. 8

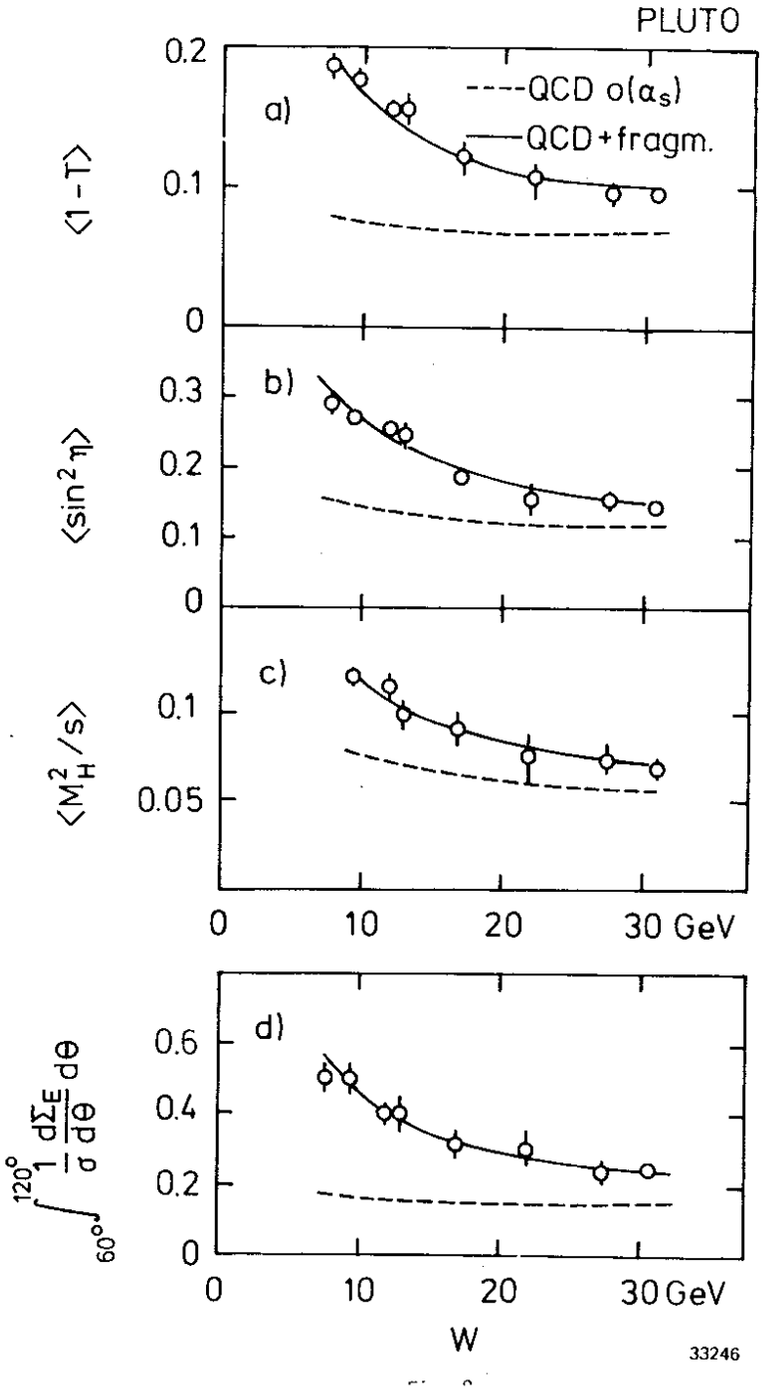
PLUTO
a)
b)
c)
d)
----QCD o(α_s)
——QCD+fragm.
⟨1 -T⟩
⟨sin²η⟩
⟨M_H²/s⟩
(1/σ) dΣ_E/dθ dθ
120°
60°
0.2
0.1
0
0.3
0.2
0.1
0
0.1
0.05
0.6
0.4
0.2
0
0
10
20
30 GeV
W
33246

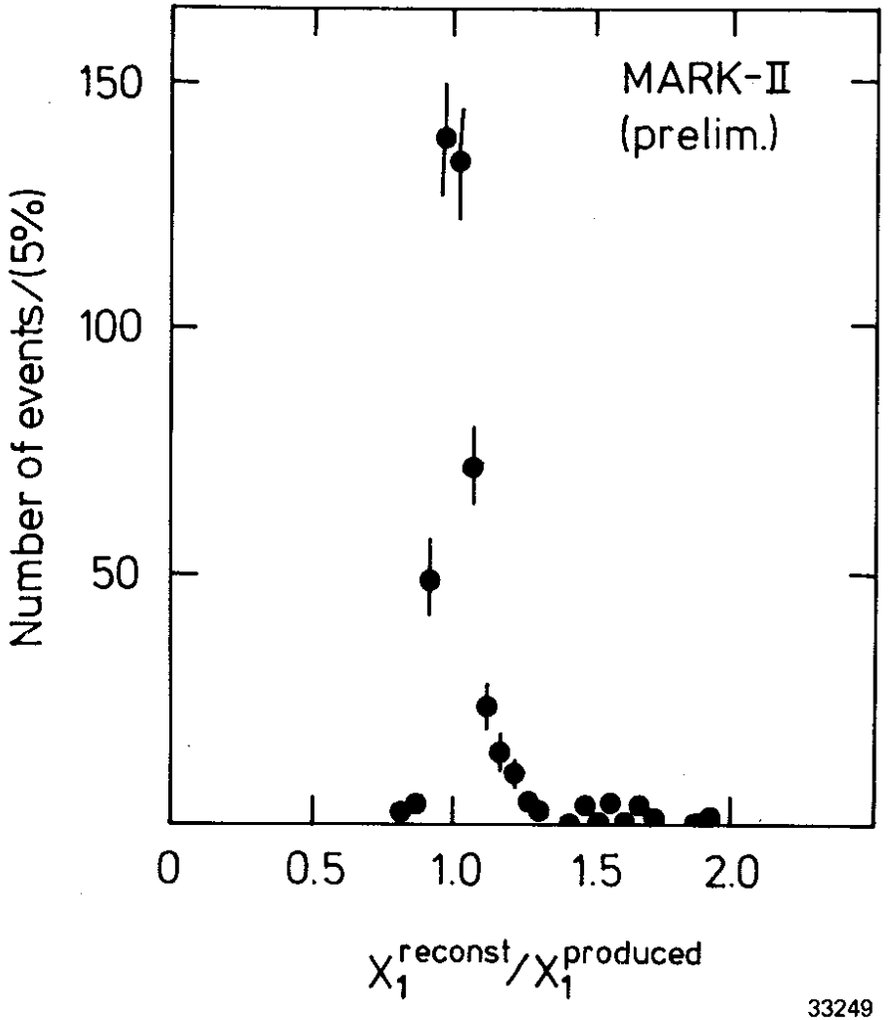
MARK-II
(prelim.)
Number of events/(5%)
150
100
50
0
0.5
1.0
1.5
2.0
X₁^reconst / X₁^produced
33249

Fig. 10

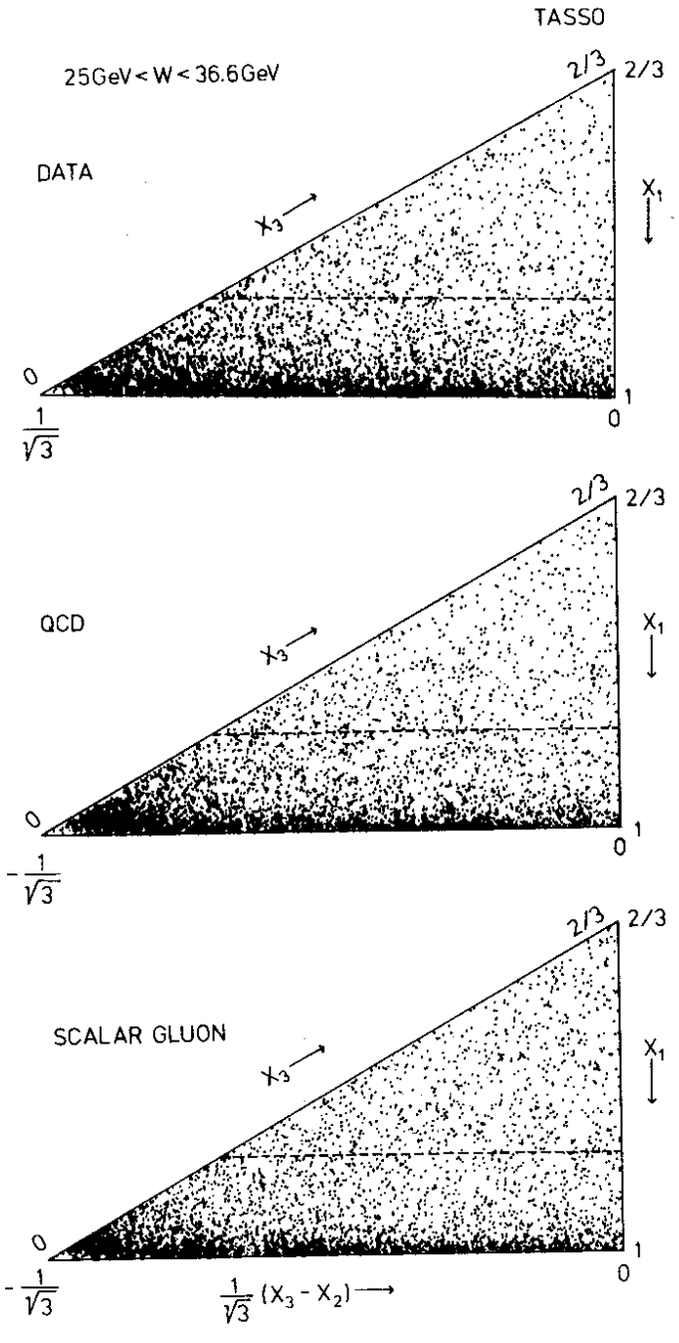

3-JET DALITZ PLOT

Fig. 11

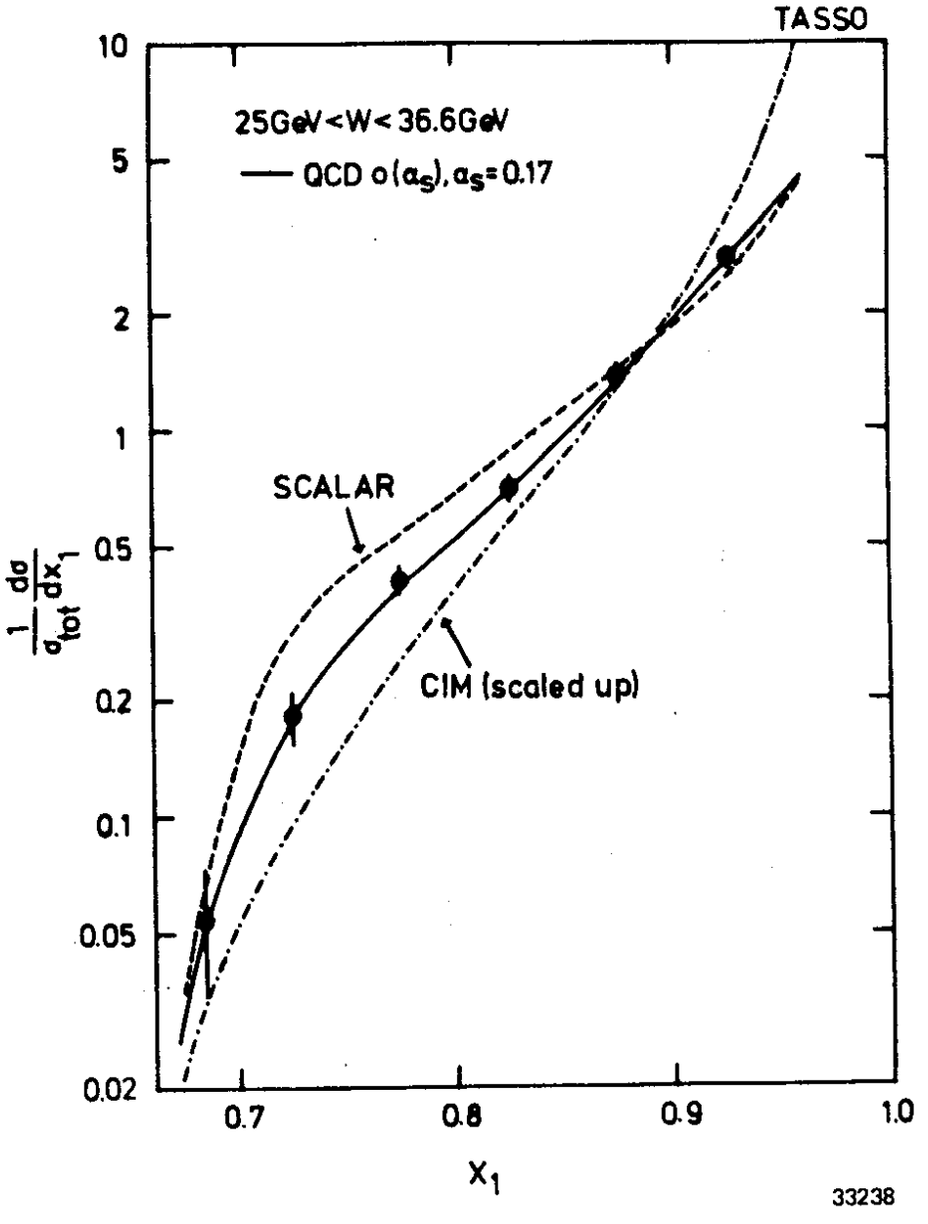

Fig. 12

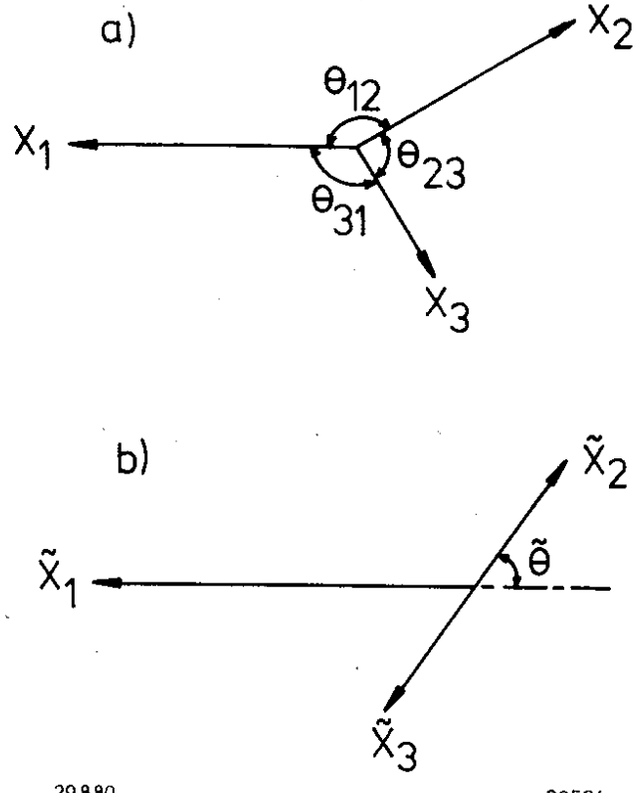
a)
X_1
X_2
X_3
θ_{12}
θ_{23}
θ_{31}
b)
$\tilde{X}_1$
$\tilde{X}_2$
$\tilde{X}_3$
$\tilde{\theta}$
29.8.80
30524

Fig. 13

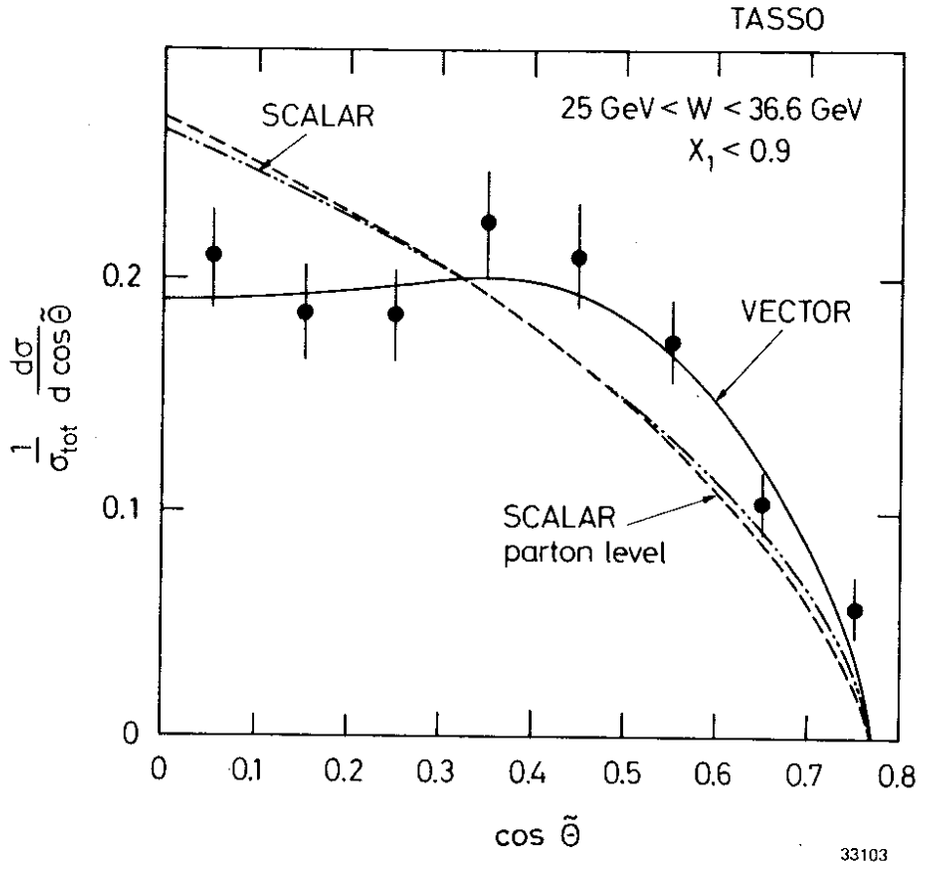
TASSO
SCALAR
25 GeV < W < 36.6 GeV
$X_1 < 0.9$
VECTOR
SCALAR
parton level
$\frac{1}{\sigma_{tot}} \frac{d\sigma}{d \cos\tilde{\Theta}}$
0
0.1
0.2
0
0.1
0.2
0.3
0.4
0.5
0.6
0.7
0.8
$\cos\tilde{\Theta}$
33103

Fig. 14

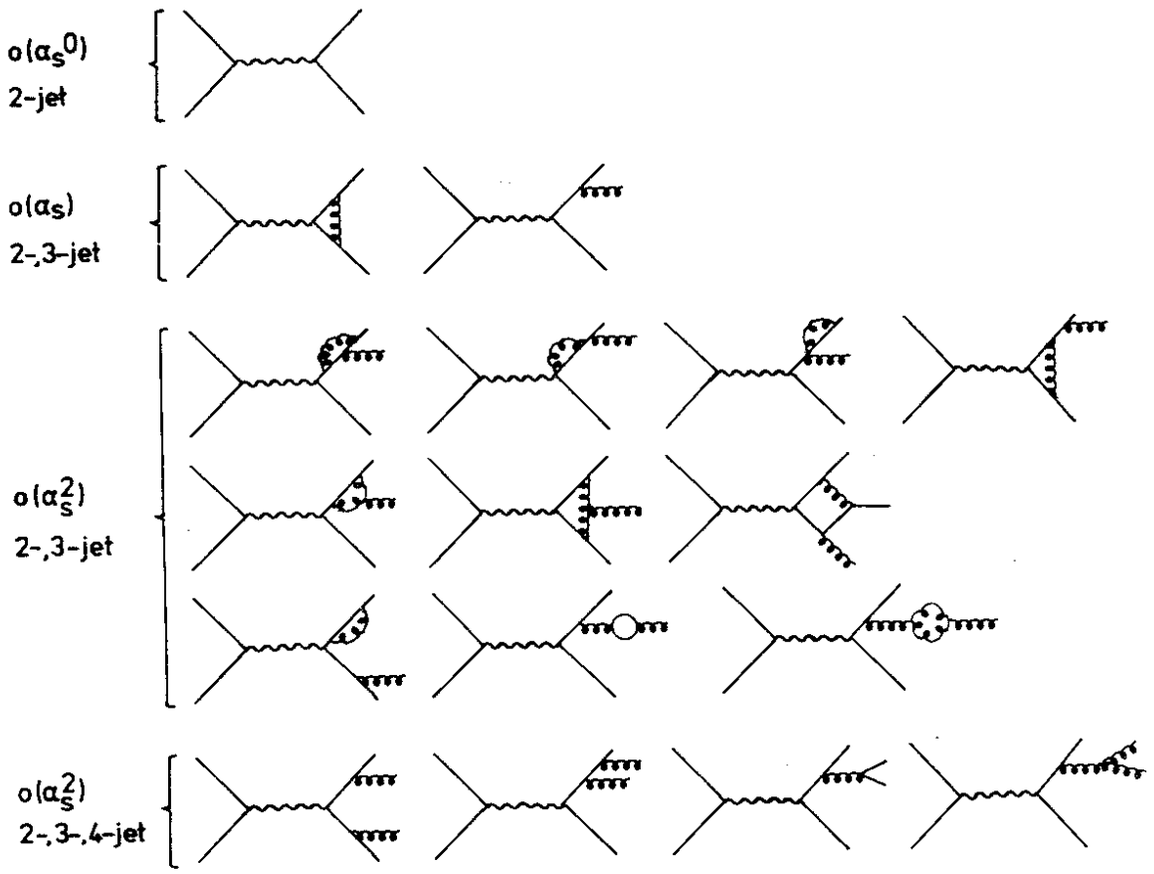

Fig. 17

33235

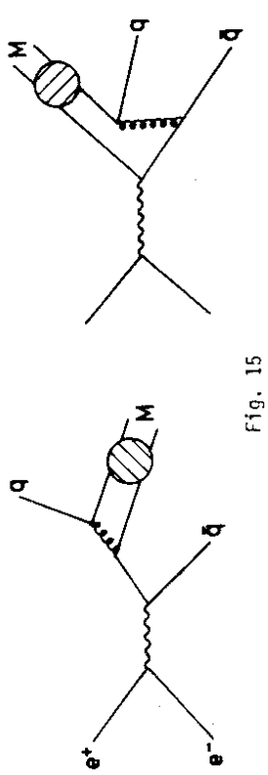

Fig. 15

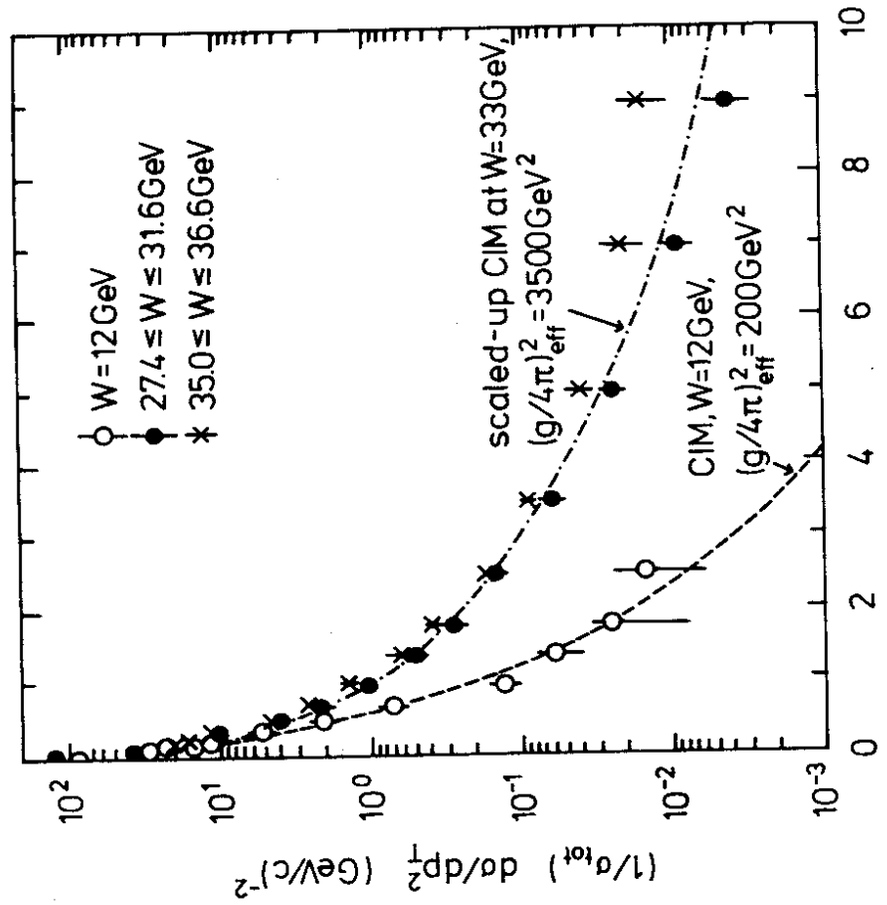

33242

Fig. 16

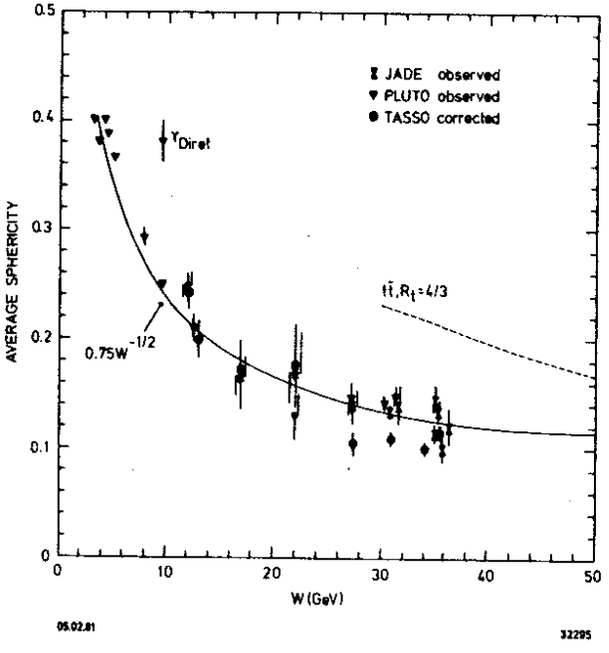
JADE observed
PLUTO observed
TASSO corrected
Υ_{Direct}
$t\bar{t}, R_t = 4/3$
$0.75W^{-1/2}$
AVERAGE SPHERICITY
W (GeV)
05.02.81
32295

Fig. 18

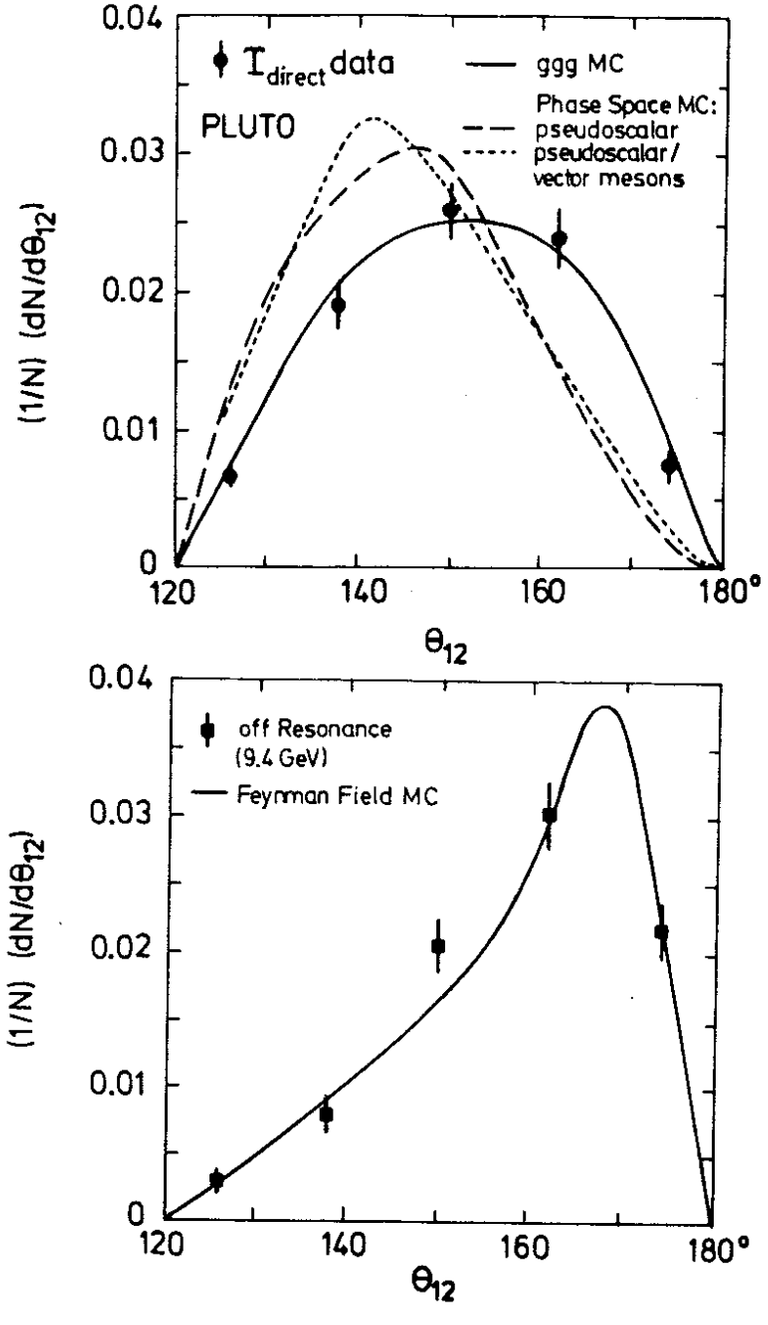
Υ_{direct} data
ggg MC
PLUTO
Phase Space MC:
pseudoscalar
pseudoscalar/
vector mesons
$(1/N)\ (dN/d\theta_{12})$
θ_{12}
off Resonance
(9.4 GeV)
Feynman Field MC

Fig. 19

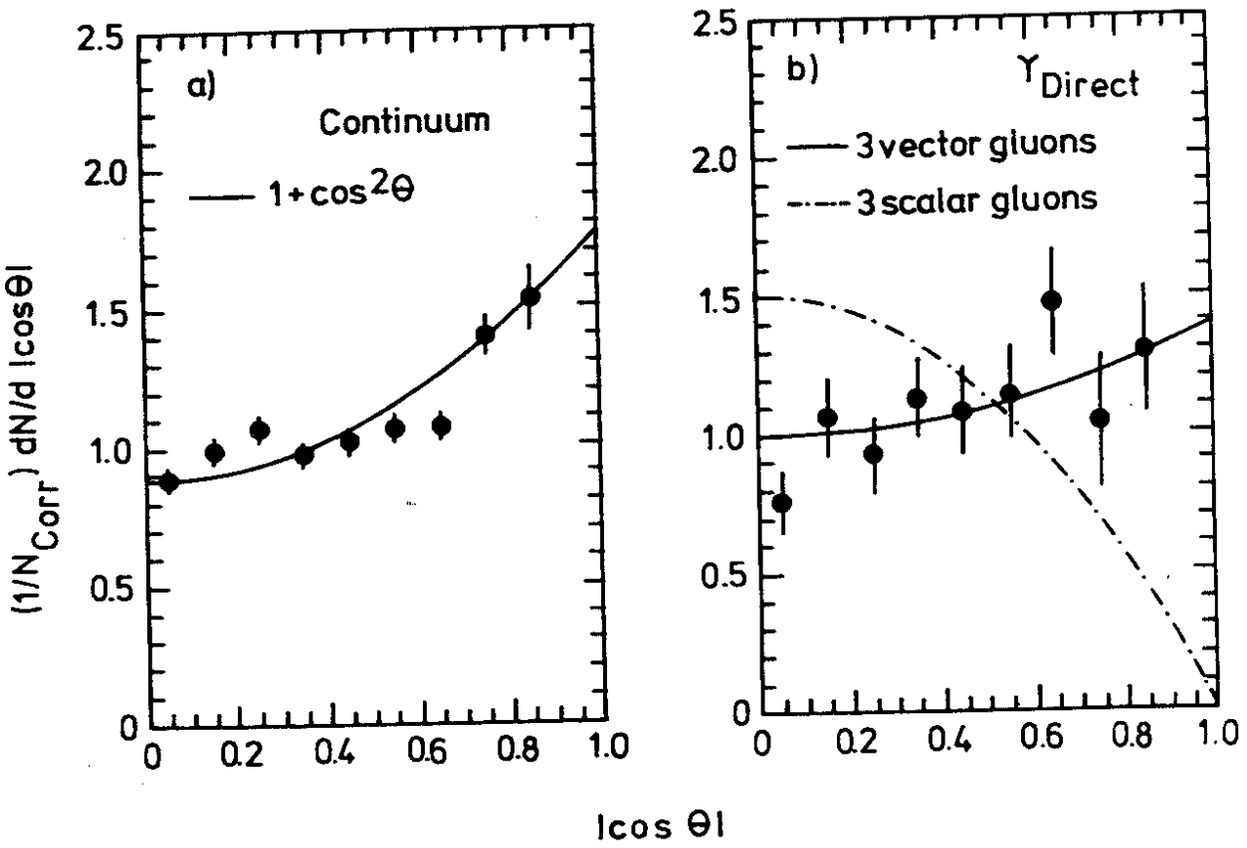

16.02.81

32296

Fig. 20